



University of  
Zurich<sup>UZH</sup>

---

---

# Pricing Catastrophe Bonds Using Extreme Value Theory

---

---

MASTER'S THESIS

SUBMITTED IN PARTIAL FULFILLMENT OF THE REQUIREMENTS FOR THE DEGREE OF MASTER OF  
ARTS IN ECONOMICS AND BUSINESS ADMINISTRATION

AUTHOR

**ALBERTO RESIDORI**

HINTERBERGSTRASSE 67, CH-8044 ZÜRICH

16-725-699

ALBERTO.RESIDORI@UZH.CH

SUPERVISOR

**PROF. DR. COSIMO-ANDREA MUNARI**

CENTER FOR FINANCE AND INSURANCE

DEPARTMENT OF BANKING AND FINANCE

UNIVERSITY OF ZURICH

DATE OF SUBMISSION: APRIL 1, 2019

This page is intentionally left blank

## **Executive Summary**

Catastrophe (CAT) bonds are financial contracts whose value is primarily driven by insurance-linked variables. Roughly speaking, the payoff of a CAT bond is contingent on an underlying index not exceeding a given threshold, known as the attachment point. Should this threshold be exceeded, the CAT bond investor loses the notional amount fully or partially and the CAT bond is said to be triggered. The index movements are typically driven by the occurrence and economic impact of natural disasters. The events on which CAT bonds are based can be classified as low frequency and high severity; for this reason, they can be analyzed and predicted in a statistically optimal manner using Extreme Value Theory (EVT).

## **Objective**

The aim of this thesis project is two-fold: first, to develop a formal arbitrage-free pricing model for CAT bonds; second, to numerically apply said model in order to evaluate an actual CAT bond deal based on insured losses from floods occurring within the United States. This thesis contributes to the scarce research on CAT bond pricing and proposes an innovative pricing approach that captures extreme events and their impact on the the CAT bond cash value.

## **Methodology**

In order to price CAT bonds as contingent claims, it is key to understand the functioning of such contracts. Hence, one chapter of this thesis is devoted to thoroughly investigating the structure of a CAT bond transaction. The CAT bond contract is then translated into mathematical terms so as to develop an analytical solution for the CAT bond price in the form of an expectation of future contingent cash flows. Given the final valuation formula, the price can be numerically approximated using Monte Carlo methods. The Monte Carlo algorithm works roughly as follows: The occurrence and size (in terms of insured losses) of flooding events are assumed to be driven by a generalized extreme value (GEV) distribution whose parameters can be estimated via a standard maximum likelihood (MLE) optimization or, subject to conditions, via the Hill (1975) approach. More specifically, statistical inference on the GEV model is drawn from a sequence of annual maximum insured losses

from floods reported by Munich Re. After obtaining a fitted GEV distribution, from which random numbers can be generated along with their impact on the CAT bond value, the price is finally determined by averaging across all simulated outcomes.

## Results

The pricing model successfully creates a final expression for the CAT bond price as the sum of discounted expectations under the risk-neutral measure, which is consistent with the no-arbitrage assumption. The numerical study starts with an EVT statistical analysis, from which it is found that the Hill estimator outperforms MLE owing to lower variance and greater accuracy in terms of in sample forecasting. Thus, the first estimation approach is chosen over the second. The CAT bond that is being evaluated consists of two tranches that, apart from the difference in the attachment point, are equivalent to each other. As expected, it is found that the tranche bearing a higher threshold is more valuable than the other, in that it is safer, i.e. less likely to be triggered. Furthermore, the numerical study produces a set of risk metrics, demonstrating how the first tranche is safer than the second.

# Contents

<b>Introduction: Research and Motivation</b>	<b>1</b>
<b>1 Overview of Insurance Securitization</b>	<b>2</b>
1.1 Sponsor's Perspective	3
1.1.1 Credit Risk	3
1.1.2 Pricing	3
1.1.3 Capital	3
1.1.4 Capacity	4
1.2 Investor's Perspective	4
1.2.1 Diversification	4
1.2.2 Low Credit and Market Risk	5
1.2.3 Investment Performance	5
1.3 Chapter Summary	6
<b>2 Structure of a CAT Bond Transaction</b>	<b>7</b>
2.1 CAT Bond Contract	7
2.2 Choice of Trigger Type	9
2.2.1 Indemnity	9
2.2.2 Industry Loss	9
2.2.3 Pure Parametric	10
2.3 Risk Sources	10
2.3.1 Basis Risk	10
2.3.2 Moral Hazard	11
2.3.3 Credit Risk	11
2.4 Sample CAT Bond Transaction	12
2.5 Chapter Summary	12
<b>3 Pricing Model</b>	<b>14</b>
3.1 Literature Review	14
3.2 Contingent Claim Pricing Model	17
3.2.1 Probabilistic Structure	17
3.2.2 Zero-Coupon CAT Bond	18
3.2.3 Introducing Coupons	20
3.2.4 Monte Carlo Pricing	22
3.3 Assumptions	22

3.3.1	Generalized Extreme Value Distribution . . . . .	23
3.3.2	Geometric Brownian Motion . . . . .	23
3.3.3	No Arbitrage and Risk Neutral Pricing Measure . . . . .	24
3.3.4	No Credit and Liquidity risk . . . . .	26
3.4	Chapter Summary . . . . .	26
<b>4</b>	<b>Extreme Value Theory</b>	<b>27</b>
4.1	Identifying Extremes . . . . .	27
4.2	Fisher, Tippett, and Gnedenko Theorem . . . . .	28
4.2.1	Generalized Extreme Value Distribution . . . . .	29
4.3	Inference on the GEV Distribution . . . . .	30
4.3.1	Maximum Likelihood Estimation . . . . .	30
4.3.2	Hill Estimator . . . . .	31
4.3.3	Other Estimators . . . . .	34
4.4	Chapter Summary . . . . .	35
<b>5</b>	<b>Numerical Study</b>	<b>36</b>
5.1	CAT Bond Deal . . . . .	36
5.2	Objective and Methodology . . . . .	38
5.3	Data . . . . .	38
5.4	Maximum Likelihood Estimation . . . . .	40
5.5	Hill Estimator . . . . .	41
5.6	Diagnostic Plots . . . . .	42
5.6.1	Density Plot . . . . .	42
5.6.2	Distribution Plot . . . . .	43
5.6.3	Q-Q Plot . . . . .	44
5.6.4	Model Selection . . . . .	45
5.7	Monte Carlo Pricing . . . . .	45
5.7.1	LIBOR . . . . .	45
5.7.2	Industry Loss Index . . . . .	47
5.8	Risk Metrics . . . . .	48
5.8.1	Exceedance Probabilities . . . . .	48
5.8.2	Return Period . . . . .	50
5.8.3	Expected Loss . . . . .	51
5.8.4	Return Level . . . . .	53
5.9	Chapter Summary . . . . .	54
	<b>Conclusion and Further Research</b>	<b>56</b>
	<b>Appendix</b>	<b>61</b>
	Appendix A Proof of Proposition 5.1 . . . . .	61
	Appendix B Approximation of the Covariance Matrix of the MLE Estimator . . . . .	62
	<b>Statement of Authorship</b>	<b>63</b>

# List of Figures

2.1	Structure of a par value CAT bond. Source: Braun (2016) . . . . .	9
5.1	Empirical (histogram) and theoretical (red line) density functions, under standard MLE approach (left panel) and Hill estimator (right panel). Source: personal research	43
5.2	Empirical (set of points) and theoretical (red line) cumulative distribution functions, under standard MLE approach (left panel) and Hill estimator (right panel). Source: personal research . . . . .	43
5.3	Q-Q plots under standard MLE approach (left panel) and Hill estimator (right panel). Source: personal research . . . . .	44
5.4	FloodSmart CAT bond price per \$100.00 of face value, evaluated at increasing attachment points (\$ billions) and exhaustion point of \$10 billion. Source: personal research . . . . .	48
5.5	Expected loss (% , left panel) and conditional expected loss (% , right panel) of the FloodSmart CAT bond, evaluated at increasing attachment points (in \$ billion) and exhaustion point of \$10 billion. Source: personal research . . . . .	52
5.6	Return level plot based on the distribution $GEV(\hat{\xi}^{Hill} = 0.6553, \hat{\mu} = 0.1502, \hat{\sigma} = 0.1593)$ . Source: personal research . . . . .	53

# List of Tables

1.1	Correlation matrix between ILS: Swiss Re CAT Bond Index, Equities: MSCI World Total Return Index , Bonds: Citigroup World Government Bond Total Return Index, Commodities: SP GSCI Total Return Index. Observation period: January 1, 2002 to March 31, 2017. Source: Lombard Odier (2017)	5
1.2	Performance summary of ILS: Swiss Re CAT Bond Index, Equities: MSCI World Total Return Index , Bonds: Citigroup World Government Bond Total Return Index, Commodities: SP GSCI Total Return Index. Observation period: January 1, 2002 to March 31, 2017. Source: Lombard Odier (2017)	6
1.3	Motivation to invest in, resp. sponsor, Insurance-Linked Securities. Source: personal research	6
2.1	Sample CAT bond transaction. Source: Swiss Re (2016)	12
5.1	CAT bond deal summary. Source: Artemis (2018)	37
5.2	Annual maximum US/Flood single-event insured losses (\$ billion). Inflation adjusted (in 2015 values). Sources: Munich Re (2018); Federal Reserve Bank of St. Louis (2018)	39
5.3	95% confidence intervals of the MLE estimates. Standard errors in parentheses. Source: personal research	40
5.4	Hill estimator. Threshold selection based on the Hall (1990) bootstrapping algorithm. Source: personal research	41
5.5	Maximum likelihood estimation for location and scale parameter, with $\xi = \hat{\xi}_{k,m}^{Hill} = 0.6553$ . Standard errors in parentheses. Source: personal research	42
5.6	Probability of exceeding the attachment, resp. exhaustion, points over multiple years, based on the distribution $GEV(\hat{\xi}^{Hill} = 0.6553, \hat{\mu} = 0.1502, \hat{\sigma} = 0.1593)$ . Source: personal research	49
5.7	Return period based on the distribution $GEV(\hat{\xi}^{Hill} = 0.6553, \hat{\mu} = 0.1502, \hat{\sigma} = 0.1593)$ , rounded to the nearest integer. Source: personal research	50
5.8	(Conditional) expected loss for the FloodSmart CAT bond. Source: personal research	52
5.9	Valuation summary. Source: personal research	55

# Nomenclature

The next list describes several of the acronyms and symbols that are later used within the body of the document

## Abbreviations

BMM	block maxima method
CEL	conditional expected loss
CIR	Cox, Ingersoll, and Ross (1985)
CPI	Consumer Price Index
DF	(cumulative) distribution function
EKM	Embrechts, Klüppelberg, and Mikosch (1997)
EL	expected loss
EVT	Extreme Value Theory
FEMA	Federal Emergency Management Agency
FRED	Federal Reserve Economic Data
GBM	geometric Brownian motion
GEV	generalized extreme value
iid	independent and identically distributed
ILS	Insurance-Linked Securities
LIBOR	London Interbank Offered Rate
MDA	maximum domain of attraction
MLE	maximum likelihood estimation
MSE	mean squared error
pdf	probability density function
POT	peak over threshold
Q-Q	quantile-quantile
SDE	stochastic differential equation

SE standard error

SPV special purpose vehicle

### Mathematical Notations

$\mathcal{F}$  natural filtration

$\mu^R$  drift of geometric Brownian motion

$\Omega$  sample space

$\mathbb{P}$  historical probability measure

$\mathbb{Q}$  risk-neutral probability measure

$\sigma^R$  volatility of geometric Brownian motion

$\tau$  stopping time

$C_0$  price

$C_t$  principal redemption

$f_n(R_n, \tau)$  coupon function

$FV$  face value, notional amount

$I_t$  triggering index

$K$  attachment point

$n = (1, 2, \dots, N)$  series of coupon dates

$p_\tau$  payout ratio to the sponsor

$r$  constant risk-free interest rate

$R_t$  LIBOR rate

$S$  spread over LIBOR

$T$  maturity date

$t$  continuous timing

$U$  exhaustion point

$W_t$  standard Brownian motion

$\mathbb{1}$  indicator function

### Statistical Notations

$\alpha$  tail index

$\bar{\Phi}_\alpha(x) = 1 - \Phi_\alpha(x)$  Fréchet tail function

$\bar{F}(x) = 1 - F(x)$  generic tail function

$\theta \in \mathbb{R}^j$  generic set of parameters

$V \in \mathbb{R}^{j \times j}$  approximate covariance matrix

$x \in \mathbb{R}^m$  block maxima

---

$\mathcal{L}(\boldsymbol{\theta}; \mathbf{x})$	likelihood function
$\mathcal{N}$	normal distribution, e.g. $\mathcal{N}(0, 1)$ denotes a standard normal with mean 0 and variance 1
$\mu$	location parameter
$\Phi_\alpha(x)$	Fréchet distribution function
$\sigma$	scale parameter
$\sim$	follows a distribution, e.g. $x \sim \mathcal{N}(0, 1)$ means that $x$ follows a standard normal distribution
$\xi$	shape parameter
$\xrightarrow{d}$	convergence in distribution
$\{x^{(i)}, i = 1, \dots, m\}$	sequence of block maxima sorted in increasing order
$\{x_{(i)}, i = 1, \dots, m\}$	sequence of block maxima sorted in decreasing order
$F(x)$	generic distribution function
$H_{\xi, \mu, \sigma}(x)$	GEV distribution function
$k$	order statistic (Hill estimator)
$k_0$	optimal order statistic (Hill estimator)
$m$	number of blocks
$u$	generic threshold
$b$	bias
$n$	block size

## Introduction: Research and Motivation

Since the first successful catastrophe (CAT) bond issuance in 1994 by the reinsurance group Hannover Re (Cummins and Weiss, 2009), these instruments have drawn the attention of scholars in the field of finance and insurance. Aside from several empirical studies, a few scholars have developed valuation frameworks for CAT bonds. Within the existing research on CAT bond pricing there is a lack of consensus. Although most of the research contributions agree with each other on some key probabilistic assumptions, the pricing models diverge significantly. This is especially noticeable in the payoff structure and in the modeled dynamics of the underlying random variables, owing to the fact that CAT bonds are very heterogeneous instruments. To address this issue, this thesis is aimed at developing a general pricing framework that can be applied to as many different types of CAT bonds as possible. A set of assumptions then restricts the model so as to numerically evaluate a specific CAT bond transaction. In particular, it is assumed that the main underlying random variable follows a distribution based on Extreme Value Theory (EVT).

The thesis is structured as follows: Chapter 1 provides background information on Insurance-Linked Securities (ILS), a broader category of financial instruments to which CAT bonds belong, as well as a short qualitative assessment of ILS from both sponsors' and investors' perspectives. In order to study in detail the pricing dynamics of a CAT bond, it is key to understand its functioning. Hence, Chapter 2 is devoted to thoroughly investigating the features of a CAT bond contract. Chapter 3 moves on to the pricing model, where the information from the previous chapter is translated into formal mathematics so as to develop a final pricing formula. Furthermore, Chapter 3 discusses the relevant literature on the subject and compares the pricing approach employed in this study against those proposed by rest of the literature. The numerical application of the pricing model requires information about the distribution of the underlying random variables. Thus, Chapter 4 introduces Extreme Value Theory and how statistical inference can be drawn from actual data, identified as extremes. Finally, Chapter 5 combines the pricing model and the statistical framework to evaluate an actual CAT bond deal based on insured losses from flooding events.

# Overview of Insurance Securitization

The National Association of Insurance Commissioners defines Insurance-Linked Securities (ILS) as securities whose performance is linked to the possible occurrence of pre-specified insurance risks. Such risks include the occurrence and impact of natural and man-made disasters as well as life-insurance variables such as longevity. Consequently, ILS are different from traditional equity and debt securities issued by insurers, in that they offer a pure play in the underlying risk types (Ammar et al., 2015). From the supply side, ILS are typically sponsored by insurers and/or reinsurers (hereafter (re)insurers), including governmental insurance programs. However, a sponsor can be any party being interested in alternative risk transfer. A prominent example is the international football association, FIFA, that sponsored a CAT bond to cover losses resulting from terror attacks and/or natural catastrophes with reference to the 2006 World Cup held in Germany (Kunreuther and Michel-Kerjan, 2009). CAT bonds are the most prominent example of ILS and cover the property and casualty segment. Other examples of ILS include industry loss warranties and, within the life and health segment, longevity bonds (see e.g. Ammar et al., 2015). As of 2018, the investor base for ILS is dominated by dedicated catastrophe funds providing 59% of capital (Aon Securities, 2018). Other categories of capacity providers include mutual and hedge funds as well as (re)insurers themselves (Aon Securities, 2018). Private investors are able to participate in the secondary ILS market by acquiring shares of dedicated ILS funds. The subsequent sections discuss the motivation to participate in the ILS market from both the sponsor's and the investor's perspective.

## 1.1 Sponsor's Perspective

The traditional way of transferring risk off balance sheet among (re)insurers is by means of reinsurance contracts<sup>1</sup>. This section briefly explains the motivation for (re)insurers to instead sponsor ILS, a form of alternative risk transfer, and under what circumstances it is preferable over traditional reinsurance.

### 1.1.1 Credit Risk

ILS are typically fully collateralized instruments. This makes them attractive when compared to traditional reinsurance, wherein the (in)solvency of the reinsuring party is a source of risk. The collateral account is typically managed by a third party, known as special purpose vehicle (SPV). The main advantage of this practice is that the solvency of the SPV is largely uncorrelated with insurance risks.

### 1.1.2 Pricing

ILS have favorable pricing as compared to reinsurance, although that depends largely on the business cycle. Indeed, after an extreme event, such as a named hurricane, reinsurance pricing tends to increase, giving rise to a "hard" market over an extended period of time (Swiss Re, 2011). During hard markets, insurers have an incentive to seek alternative sources of risk financing and, since CAT bonds are traded daily in the secondary market, risk pricing is more flexible and responds faster to market conditions than traditional reinsurance. Furthermore, once a (re)insurer sponsors an ILS at a favorable pricing, it can take advantage of the coverage over a multiyear period. On the other hand, reinsurance contracts are typically renewed yearly under new terms (Swiss Re, 2011).

### 1.1.3 Capital

Similar to reinsurance, sponsoring ILS allows a (re)insurer to decrease its minimum capital requirements, thereby boosting the return on equity and/or allowing the relaxation of regulatory as well as

---

<sup>1</sup> Here "reinsurance" refers to both reinsurance contracts for insurers and retrocession contracts for reinsurers.

internal underwriting constraints. The capital relief is even greater for ILS that cover multiple perils (Swiss Re, 2011).

#### 1.1.4 Capacity

Securitization not only benefits (re)insurers individually but also the industry as a whole. Indeed, capital markets have a much greater capacity of bearing risk than the (re)insurance industry. It is estimated that, in 2005, the hurricanes Katrina, Rita, and Wilma and other events combined caused insured losses of \$114 billion. This amount, while large relative to the total equity capital of global (re)insurers combined, represents less than 0.5% of the value of the US stock and bond markets alone (Cummins and Weiss, 2009, p. 494).

## 1.2 Investor's Perspective

This section outlines the role of ILS as an alternative asset class and what makes them attractive to the investor in terms of performance and diversification benefits.

### 1.2.1 Diversification

It is generally accepted that the ILS market provides investors with an attractive risk-return profile while maintaining its diversification benefits. Cummins and Weiss (2009) studied this phenomenon in detail and concluded that ILS are barely correlated to other asset classes under normal economic conditions. The same authors, however, concluded that ILS are significantly correlated with equities and corporate bonds under financial crisis scenarios and, therefore, subject to systemic risk, like all other asset classes. Table 1.1, taken from Lombard Odier (2017), illustrates the cross-asset correlation between ILS and other main asset classes.

**Table 1.1** – Correlation matrix between ILS: Swiss Re CAT Bond Index, Equities: MSCI World Total Return Index, Bonds: Citigroup World Government Bond Total Return Index, Commodities: SP GSCI Total Return Index. Observation period: January 1, 2002 to March 31, 2017. Source: Lombard Odier (2017)

	ILS	Equities	Bonds	Commodities
ILS	1			
Equities	0.18	1		
Bonds	0.12	0.16	1	
Commodities	0.11	0.40	0.18	1

### 1.2.2 Low Credit and Market Risk

Aside from the low systematic risk, ILS are structured so as to be largely immune to other typical financial risks. ILS typically pay a fixed spread plus a floating component based on a certain reference rate. This minimizes the interest rate risk. Moreover, ILS are typically fully collateralized instruments and are structured so that the solvency of the sponsoring party does not impact the repayment of the contractual obligations<sup>2</sup>. Adding that to high collateral standards, credit risk is largely eliminated. In summary, ILS are designed to bear insurance risk only; in other words, they offer a pure-play in the underlying insurance-linked variables.

### 1.2.3 Investment Performance

ILS are not only attractive as a diversification tool but they also perform relatively well as a stand alone asset class. Indeed, several empirical studies demonstrate that ILS consistently outperform other traditional asset classes. Table 1.2, taken from Lombard Odier (2017), reports a short performance summary of ILS along with other main asset classes.

<sup>2</sup> More details will follow in the next chapter

**Table 1.2** – Performance summary of ILS: Swiss Re CAT Bond Index, Equities: MSCI World Total Return Index, Bonds: Citigroup World Government Bond Total Return Index, Commodities: SP GSCI Total Return Index. Observation period: January 1, 2002 to March 31, 2017. Source: Lombard Odier (2017)

Asset class	Annualized return	Annualized volatility	Sharpe ratio
ILS	8.00%	2.70%	2.23
Equities	6.20%	15.20%	0.36
Bonds	4.80%	6.90%	0.48
Commodities	-1.30%	23.30%	N/A

According to the above table, ILS dominate the other asset classes, as they outperform their counterparts in every item.

### 1.3 Chapter Summary

Insurance-Linked Securities are an attractive means of alternative risk transfer for sponsors and offer an outstanding performance to institutional investors, characterized by a favorable risk-return profile as well as low correlation to other asset classes. Table 1.3 summarizes the motivation to invest in, resp. sponsor, Insurance-Linked Securities discussed in this chapter.

**Table 1.3** – Motivation to invest in, resp. sponsor, Insurance-Linked Securities. Source: personal research

Motivation to invest in	Motivation to sponsor
Low correlation with other asset classes	Risk bearing capacity
Performance	Favorable pricing
Low credit and interest rate risk	Multiyear coverage

## Structure of a CAT Bond Transaction

In order to develop a pricing model for CAT bonds, it is key to understand the functioning of such instruments. Hence, this chapter is devoted to thoroughly investigating how a CAT bond deal is structured. In particular, the next sections examine the conditions under which investors lose their capital and how the sponsor is compensated in case a triggering event occurs.

### 2.1 CAT Bond Contract

A CAT bond contract involves three main parties: the *sponsor*, the *investor*, and a *special purpose vehicle* (SPV). The SPV plays three important roles. First, it issues the CAT bond to the investor and allocates the proceeds from the sale to a collateral account. Second, it collects the fixed *spread* payments from the sponsor and the floating-rate payment generated from the collateral fund. Floating-rate payments are based on a benchmark interest rate, such as the London Interbank Offered Rate (LIBOR). Lastly, the SPV pays to the investor periodic coupons, which consist of the two components mentioned above, as well as the full principal at maturity in case no qualifying triggering event occurs. A CAT bond is said to be *triggered* if a qualifying event causing an index value to exceed a predefined *attachment point* occurs before or at maturity. The occurrence of a single or multiple qualifying events is a necessary but not sufficient condition for the CAT bond to be triggered. Reasons for this include but are not limited to the following:

1. It is possible that a qualifying event occurs no later than the maturity date, but the resulting index value does not reach the threshold.
2. The CAT bond can only be triggered by a single event; hence, multiple index values below the threshold cannot trigger the CAT bond even if they exceed the threshold when combined<sup>3</sup>.
3. A single qualifying event that causes an index value above the attachment point may only occur after maturity.

To objectively determine how an event qualifies and how its occurrence may trigger the CAT bond, the contract must specify the following information (Braun, 2012):

1. Reference peril(s). Can be natural catastrophe (e.g. earthquakes, typhoons, hurricanes, floods and so on), or man-made disasters (e.g. terror and cyber attacks)
2. Geographical region(s) potentially affected by the reference peril(s).
3. Trigger type (indemnity, industry loss or pure parametric), a measure for the index value associated with the qualifying event.

In case the CAT bond is triggered, the sponsor ceases to make spread payments, and the SPV liquidates the principal. The proceeds from the sale are split between the investor and the sponsor. The residual principal paid to the sponsor increases proportionally with the difference between the index value and the attachment point<sup>4</sup>. Once the index value reaches the *exhaustion point*, a second pre-specified threshold greater than the attachment point, the investor loses the entire principal, as the full amount is transferred to the sponsor. However, the investor cannot lose more than the notional amount, even if the index exceeds the exhaustion point. The diagram in figure 2.1 represents a CAT bond issued at par, i.e. the face value is equal to the price paid by the investor.

---

<sup>3</sup> A CAT bond can be structured to provide cover for a single event (per occurrence cover) or to provide aggregate cover for multiple events (Artemis, nd). In this framework, however, only per occurrence covers have been considered.

<sup>4</sup> Both binary and proportional payoffs are possible, although the latter is mostly the case (Cummins and Weiss, 2009, p. 523). In this framework, the CAT bond bears a proportional payoff with respect to the principal, while coupon payments follow a binary structure.

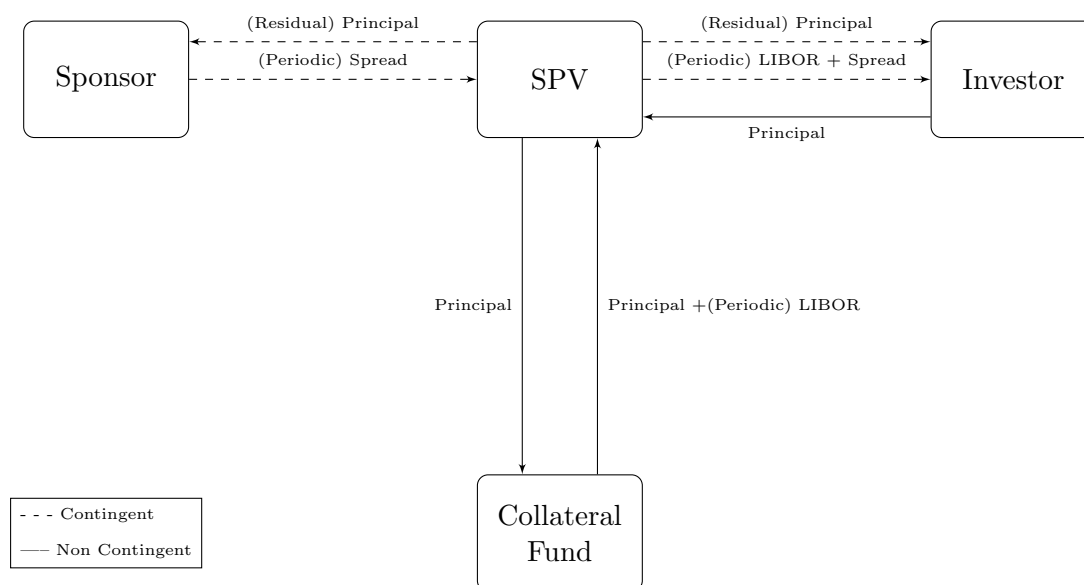


**Figure 2.1** – Structure of a par value CAT bond. Source: Braun (2016)

## 2.2 Choice of Trigger Type

With reference to the previous section, the trigger type is extremely relevant in order to objectively determine how a qualifying event may trigger a CAT bond and what fraction of the notional amount is transferred to the sponsor. Hence, the choice of trigger type must be contractually specified. This section discusses the most common options.

### 2.2.1 Indemnity

Indemnity-based contracts dominate the CAT bond market with a primary issuance volume in the first quarter of 2018 (Q1-2018) of \$4.649 billion (Swiss Re, 2018). Indemnity triggers are based on the individual losses reported by the sponsor as a result of a qualifying event.

### 2.2.2 Industry Loss

CAT bonds based on an industry loss trigger account for a primary issuance volume of \$1.3 billion as per Q1-2018 (Swiss Re, 2018). Industry loss triggers are based on insured losses that result from a qualifying event. In other words, the industry loss index reports how much the entire (re)insurance industry lost as a result of a particular event. The overall industry losses are never known with

certainty. Estimates are produced by third party agencies collecting claim reports from as many worldwide (re)insurers as possible. Thus, in case of an industry loss trigger, the CAT bond contract must additionally specify the third party agency reporting the loss estimate. The most widely accepted service providers are Property Claim Services from Verisk Analytics and PERILS.

### **2.2.3 Pure Parametric**

During Q1-2018, CAT bonds with a pure parametric trigger were issued for a total volume of \$1.36 billion (Swiss Re, 2018). Pure parametric are popular among investors, as they offer the highest degree of transparency. They are based on the physical parameters recorded following a natural catastrophe (such as wind speed, earthquake magnitude, and so on). Unlike individual or industry losses, data on physical parameters are publicly available, allowing for the transparency.

## **2.3 Risk Sources**

Aside from the obvious insurance-linked risk CAT bonds are subject to, this section discusses other sources of risk from the perspective of both sponsors and investors.

### **2.3.1 Basis Risk**

In the context of ILS, basis risk refers to the discrepancy between the actual losses incurred by the sponsor and the recovery provided by the CAT bond following a qualifying event. In other words, basis risk arises from the possibility that the compensation received according to the contractual terms of the CAT bond may not suffice to cover the actual losses incurred by the sponsor. Indemnity-based CAT bonds minimize basis risk, whereas pure parametric maximize such risk. A sponsor would agree on an industry loss trigger only under the expectation that its individual losses are positively correlated to those of the overall (re)insurance industry (Lee and Yu, 2002).

### 2.3.2 Moral Hazard

Moral hazard occurs when a party increases its risk exposure, under the assurance that another party bears a part or the full cost of such a risk. In the context of CAT bonds, moral hazard opportunities arise when the sponsor's cost of loss control efforts exceeds the benefits from debt forgiveness (Lee and Yu, 2002). That is, the sponsor as a (re)insurer has an incentive to relax its underwriting constraints and gain a higher risk exposure, given the protection provided by the CAT bond contract. Indemnity-based triggers therefore maximize the moral hazard occurrence, given that the size of the catastrophic event is self-reported by the sponsor. Industry loss triggers minimize the risk of moral hazard at the individual level. However, opportunities still persist, in that the insurance claims are self-reported by the industry (Braun, 2012). However, sponsors, whether individually or as a group, have no influence over the reporting of physical parameters of the natural catastrophes; hence, pure parametric triggers eliminate moral hazard opportunities.

### 2.3.3 Credit Risk

Credit risk refers to the possibility that the CAT bond's counter-parties might default on their contractual obligations, adversely affecting the principal redemption by the investor. CAT bonds are structured so that the (in)solvency of the sponsor does not impact the principal redemption by the investor. Nevertheless, sources of credit risk may arise from weaknesses in the structure of the collateral account. During the financial crisis, four CAT bonds defaulted as a result of a pure credit event, namely the bankruptcy of Lehman Brothers (Towers Watson, 2010). The investment bank acted as a total return swap counter-party to the collateral fund, and its bankruptcy caused the downgrading and the technical default of the four CAT bonds. After the financial crisis, however, improvements were made to collateral standards, including the abandoning of the total return swap structure, which decreased credit risk in CAT bonds even further (Towers Watson, 2010). For this reason, CAT bonds can be assumed to be default-free securities, which is in line with most of the existing literature.

## 2.4 Sample CAT Bond Transaction

Table 2.1 provides a sample CAT bond transaction. Note that key information (attachment and exhaustion point) is missing. Nevertheless, the following table is useful in complementing the information presented earlier in this chapter.

**Table 2.1** – Sample CAT bond transaction. Source: Swiss Re (2016)

<b>First Coast Re Ltd. 2016-1 A</b>	
Sponsor	Security First Insurance Company
SPV	First Coast Re Ltd.
Issuance date	June 1, 2016
Maturity date	May 31, 2019
Territory/Peril	Florida/storm or sever thunderstorm
Trigger Type	Indemnity, per occurrence
Notional	USD 75 million

## 2.5 Chapter Summary

A CAT bond contract must specify the following key information:

1. Maturity
2. Spread and coupon structure (e.g. annual)
3. Reference floating interest rate (e.g. LIBOR)
4. Reference territory (single or multiple) and peril (single or multiple)
5. Trigger type (single or combination of multiple)
6. Attachment point

### 7. Exhaustion point

CAT bonds are very heterogeneous instruments in that they vary greatly in their structure based on the items listed above. However, one common feature of all CAT bond transactions is that they are structured in a manner that the (in)solvency of the sponsoring party does not impact the repayment of the principal, thereby minimizing counter-party credit risk. One of the most relevant decision criteria when structuring a CAT bond deal is the choice of trigger type. This represents a trade-off between transparency (from the investor's perspective the higher the better) and basis risk (the lower the better from the sponsor's perspective).

## Pricing Model

Catastrophe (CAT) bonds can be thought of as contingent claims, in that their payoff is contingent on an underlying natural catastrophe process not exceeding a given threshold. Unlike traditional derivative contracts, CAT bonds are priced in an incomplete market framework, that is, the underlying triggering process is not linked to a tradable financial asset. Hence, it is not possible to construct a portfolio of assets that replicates the CAT bond payoff. The next section discusses the existing research on the pricing of such instruments and how the previous contributions addressed the problem of incomplete markets. Furthermore, the next section compares the approach adopted in this thesis to those proposed by the existing literature. This chapter then moves on to the pricing model and the related assumptions.

### 3.1 Literature Review

The existing literature on CAT bonds pricing model is divided in two approaches, namely econometric and contingent claim. Econometric approaches base their pricing model on a large sample of data of actual CAT bond transactions and determine the CAT bond spread as a linear function of several other variables by means of an ordinary least square regression. One of the explanatory variables of interest is the CAT bond reported expected loss, which is found to be statistically significant by several studies (see e.g. Bodoff and Gan, 2009; Braun, 2016).

In contrast to econometric models, contingent claim approaches are more focused on the CAT bond price rather than the spread, which is typically given as a constant. Contingent claim pricing models typically consist of first developing a formal mathematical model for the CAT bond price and then applying the model numerically by means of Monte Carlo simulations, given that often there is no closed-form solution for the price.

**Cox and Pedersen (2000)** propose a discrete arbitrage-free pricing model. In this model, there are two types of random variables, those depending only on natural catastrophes and those depending only on financial markets. Under the historical probability measure, the two types of variables are assumed to be independent of each other. The two authors then show that when switching from the historical to the risk-neutral probability measure the two types of variables retain independence. Furthermore, they show that the expectation of a variable that depends only on catastrophic risk is the same under the historical and risk-neutral measure. Another important conclusion of the work by Cox and Pedersen (2000) is that imposing no-arbitrage in incomplete markets would only restrict the price of a CAT bond to a range of possible arbitrage-free values. Indeed, market incompleteness implies that the risk-neutral measure is not unique and hence the price is not uniquely defined.

Most of the subsequent literature extends the probabilistic framework by Cox and Pedersen (2000) to a continuous<sup>5</sup> setting and retains the no-arbitrage framework, with the exception of Zimbidis et al. (2007) as well as the independence assumption, with the exception of Nowak and Romaniuk (2018).

**Lee and Yu (2002, 2007)** develop a model in which CAT bonds are directly issued by the sponsor. It follows that CAT bonds are subject to credit risk, as the solvency of the issuing party directly impacts the CAT bond payoff. Default risk is investigated via the asset and liability dynamics. Additional sources of risk are represented by the interest rate, which is driven by the CIR (Cox, Ingersoll, and Ross, 1985) model, a mean reverting process, which includes a Brownian component. The underlying catastrophe index (industry loss) follows a compound Poisson process.

**Vaugirard (2003a,b)** models the dynamics of the underlying index via a Merton (1976) jump-diffusion process. This process includes a Brownian component representing ordinary index movements and a Poissonian part representing large discontinuous movements; these are known as *jumps*.

---

<sup>5</sup> The Cox and Pedersen (2000) framework is both time and space-discrete, in that there is a finite number of states in the economy.

Catastrophic events are seen as jumps in the underlying index and are assumed to be unsystematic, i.e. fully diversifiable. It follows that investors are neutral towards catastrophic risk. Furthermore, it is assumed that ordinary index movements can be replicated by existing securities. Based on these two assumptions, Vaugirard (2003a,b) shows the existence of a well-defined arbitrage-free price, in stark contrast to the solution proposed by Cox and Pedersen (2000).

The actuarial approach by **Zimbidis, Frangos, and Pantelous (2007)** distinguishes itself from the rest of the literature in that it is entirely based on the historical probability measure. Furthermore, the underlying index process (earthquake magnitude) is a sequence of independent and identically distributed (iid) random variables whose distribution is based on Extreme Value Theory.

In contrast to other models which are solved via numerical approximations, the valuation formula proposed by **Jarrow (2010)** admits a closed-form solution for the price. This approach is based on reduced form models used to price credit derivatives and is consistent with the no-arbitrage framework.

**Nowak and Romaniuk (2013)** extend the approach employed by Vaugirard (2003a) to a more general pricing framework, where the interest rate dynamics are modeled as a Vasicek (1977), Hull and White (1990) and CIR process.

Recently, **Nowak and Romaniuk (2018)** have relaxed the independence assumption by introducing a non-zero correlation factor between two Brownian motions—one belonging to the interest rate CIR dynamics and the other belonging to the jump-diffusion process for the underlying index.

This thesis distinguishes itself from most of the existing literature, in that the index dynamics are represented by a sequence of iid random variables with a common distribution function based on Extreme Value Theory. Unlike most of the literature, the triggering process is based on single events rather than the sum of consecutive events. This application of EVT has several advantages over the traditional compound Poisson process when modeling catastrophic events. First of all, under certain conditions, the arrival of catastrophic events is deterministic and only the size of such events is random. Indeed, under the block maxima method, extremal events are expected to occur at a fixed frequency. Furthermore, EVT allows to easily determine relevant statistics via a closed-form

solution. Examples of this include but are not limited to the following:

1. Probability of the underlying index exceeding a given threshold (e.g. the CAT bond attachment point) within a given period (e.g. the CAT bond maturity)
2. Expected period needed to observe an index value exceeding a given threshold (return period)
3. Expected threshold to be exceeded within a given period (return level)

Further, this thesis assumes that the risk-free interest rate is constant for discounting purposes. On the other hand, the LIBOR rates, which directly impact coupon payments, are assumed to be driven by a geometric Brownian motion, as seen in Zimbidis et al. (2007) and Romaniuk (2003). This thesis is loosely based the approach used by Zimbidis et al. (2007). However, there is a substantial difference between the two. Unlike the reference paper, this thesis adopts the no-arbitrage approach when pricing CAT bonds; thus, the expected value of the CAT bond payoff is determined under the risk-neutral measure. This divergence is especially noticeable in that the approach employed in this thesis determines the CAT bond expected return as the risk-free rate, whereas the approach by Zimbidis et al. (2007) attaches a risk premium to the discount rate.

## 3.2 Contingent Claim Pricing Model

This section develops a formal arbitrage-free pricing model for the CAT bonds, which is loosely based on previous contributions. In particular, the probabilistic framework follows roughly that of Cox and Pedersen (2000), while the underlying index and interest rate dynamics are similar to those in Zimbidis et al. (2007).

### 3.2.1 Probabilistic Structure

In this framework, there are two types of random variables. The natural catastrophe, or insurance, variables are governed by the probability space:

$$(\Omega_1, \mathcal{F}_1, \mathbb{P}_1)$$

where the three entries denote the state space, the natural filtration, and the historical probability measure respectively. Similarly, financial market variables are governed by the triple:

$$(\Omega_2, \mathcal{F}_2, \mathbb{Q}_2)$$

Unlike  $\mathbb{P}_1$ ,  $\mathbb{Q}_2$  is a risk-neutral pricing measure. Later in this chapter, the relationship between historical and risk-neutral probabilities is thoroughly discussed in subsection 3.3.3. The probability space of the full model is denoted by the triple given below:

$$(\Omega, \mathcal{F}, \mathbb{Q})$$

Under  $\mathbb{Q}$  natural catastrophe and financial market variables are assumed to be independent. This assumption is consistent with most of the existing literature on CAT bond pricing and can be formalized following Cox and Pedersen (2000). A generic element (state) of the sample space  $\Omega = \Omega_1 \times \Omega_2$  takes the following form:

$$\omega = (\omega_1, \omega_2) \quad \omega_1 \in \Omega_1 \quad \omega_2 \in \Omega_2$$

The probability of a generic state  $\omega$  occurring is assumed to be given by the following product structure:

$$\mathbb{Q}(\omega) = \mathbb{P}_1(\omega_1) \mathbb{Q}_2(\omega_2)$$

The above identity implies that the realization of state  $\omega_1$  is independent of the realization of state  $\omega_2$ . In other words, the above identity formally implies the independence between catastrophic and financial risks.

### 3.2.2 Zero-Coupon CAT Bond

The pricing of the zero-coupon CAT bond only depends on the insurance variables governed by the probability space  $(\Omega_1, \mathcal{F}_1, \mathbb{P}_1)$ . A zero-coupon CAT bond pays its holder the face value  $FV$  at maturity  $T$  contingent on the index process  $(I_t)_{t \geq 0}$ , a stochastic process under  $\mathbb{P}_1$ , not exceeding

the attachment point  $K$  before or at maturity date. Otherwise, if the CAT bond is triggered, the investor redeems only a fraction of the principal. The CAT bond payoff can be expressed as the sum of two contingent and mutually exclusive payments:

$$C_T + C_\tau \tag{3.1}$$

where the first component  $C_T$  is the contingent payoff at maturity and is defined as follows:

$$C_T = FV\mathbb{1}_{\tau > T} \tag{3.2}$$

The stopping time  $\tau$  of the process  $(I_t)_{t \geq 0}$  is a random variable  $\tau : \Omega_1 \rightarrow [0, \infty)$ , formally determined in (3.3).

$$\tau = \inf\{t \in [0, \infty) : I_t \geq K\} \tag{3.3}$$

In other words,  $\tau$  is the first date at which the index reaches the threshold  $K$ , which may occur before, at, or after maturity. If and only if  $\tau > T$ , the CAT bond is not triggered. This statement is expressed by means of the indicator function  $\mathbb{1}_{\tau > T} : \Omega_1 \rightarrow \{0, 1\}$ , which is determined as follows:

$$\mathbb{1}_{\tau > T} = \begin{cases} 1, & \text{if } \tau > T \\ 0, & \text{if } \tau \leq T \end{cases} = 1 - \mathbb{1}_{\tau \leq T} \tag{3.4}$$

The principal redemption at its full nominal value is conditional on the triggering event occurring later than maturity. However, given that the CAT bond can be triggered at any time before or at maturity, it is necessary to account for the scenario under which  $\tau \leq T$ . The payoff of the zero-coupon CAT bond liquidated before maturity is determined as follows:

$$C_\tau = (1 - p_\tau)FV\mathbb{1}_{\tau \leq T} \tag{3.5}$$

where the payout ratio  $p_\tau$  to the sponsor is a random variable  $p_\tau : \Omega_1 \rightarrow [0, 1]$  whose value is determined as follows:

$$p_\tau = \begin{cases} 0, & \text{if } \tau > T \\ \frac{I_\tau - K}{U - K}, & \text{if } \tau \leq T \wedge K \leq I_\tau \leq U \\ 1, & \text{if } \tau \leq T \wedge I_\tau > U \end{cases} \quad (3.6)$$

where the exhaustion point  $U > K$  is a contractually specified threshold. Note that in the limiting case in which  $U = K$ , the principal redemption reduces to a binary payoff structure. Finally, the price of the zero-coupon CAT bond  $C_0$  is given in (3.7) as the present value of the expected payoff under the two mutually exclusive scenarios described in equations (3.2) and (3.5).

$$C_0 = B(T, r) \mathbb{E}_{\mathbb{P}_1} [C_T] + \mathbb{E}_{\mathbb{P}_1} [B(\tau, r) C_\tau] \quad (3.7)$$

Here,  $\mathbb{E}_{\mathbb{P}_1}$  denotes the expected value under  $\mathbb{P}_1$ . The continuous time discount factor  $B(t, r)$  is based on a constant risk-free interest rate  $r$  and is given by (3.8). Note that  $r$  should not be confused with the LIBOR rate  $R_t$ , a random variable defined in the next subsection.

$$B(t, r) = e^{-rt} \quad (3.8)$$

### 3.2.3 Introducing Coupons

The payoff of a coupon paying CAT bond is determined by both the LIBOR and the natural catastrophe process. Hence, the pricing dynamics are governed by the probability space for the full model  $(\Omega, \mathcal{F}, \mathbb{Q})$ . In particular, the LIBOR evolution is represented by the stochastic process  $(R_t)_{t \geq 0}$  under  $\mathbb{Q}_2$ . A coupon CAT bond pays a stream of contingent cash flows up until the maturity date  $T$ . The coupon payment dates are represented by the series  $n = (1, 2, \dots, N)$ . From date  $n = 1$  to  $n = N - 1$ , the investor receives either the coupon payment, which is conditional on the CAT bond not being triggered, or the residual principal, in case the CAT bond is triggered. At maturity  $N$ , the principal is repaid at its full nominal value along with the last coupon payment, conditional on the bond not being triggered before or at maturity. While the underlying triggering event can occur continuously at any point in time, the repayment of the residual principal only takes place at the next coupon

date, i.e., if  $\tau \in (n-1, n]$ , the residual principal is paid at date  $n$ . The principal redemption  $C_n$  in (3.9) is determined analogously as in equation (3.5):

$$C_n = \begin{cases} (1 - p_\tau)FV\mathbb{1}_{\tau \in (n-1, n]}, & \text{if } n < N \\ (1 - p_\tau)FV\mathbb{1}_{\tau \in (N-1, N]} + FV\mathbb{1}_{\tau > N}, & \text{if } n = N \end{cases} \quad (3.9)$$

where  $p_\tau$  is determined as in the previous section, except that  $N$  replaces  $T$ . The coupon at date  $n$  is composed of the (random) LIBOR-based interest payment  $R_n FV$ , i.e. the  $n$  realization of the LIBOR process  $(R_t)_{t \geq 0}$  scaled by the notional amount  $FV$ , and the fixed spread payment  $S$  collected from the sponsor. The contingent coupon cash flow is determined as follows:

$$f_n(R_n, \tau) = (R_n FV + S)\mathbb{1}_{\tau > n} \quad (3.10)$$

The full cash flow is expressed in (3.11) as the sum of coupon and principal redemption. Note that, for  $n < N$ , the two components are mutually exclusive.

$$f_n(R_n, \tau) + C_n \quad (3.11)$$

The price of the CAT bond is finalized as the sum of the present values of the expected cash flows. The expected value is determined under the probability measure for the full model  $\mathbb{Q}$ .

$$C_0 = \sum_{n=1}^N B(n, r) \mathbb{E}_{\mathbb{Q}} [f_n(R_n, \tau) + C_n] \quad (3.12)$$

The expectation in (3.12) can be linearly decomposed as follows:

$$\begin{aligned} & \mathbb{E}_{\mathbb{Q}} [f_n(R_n, \tau) + C_n] \\ &= \mathbb{E}_{\mathbb{Q}} [f_n(R_n, \tau)] + \mathbb{E}_{\mathbb{Q}} [C_n] \\ &= \mathbb{E}_{\mathbb{Q}} [(R_n FV + S)\mathbb{1}_{\tau > n}] + \mathbb{E}_{\mathbb{Q}} [C_n] \end{aligned} \quad (3.13)$$

As established earlier in this chapter, the random variable  $C_n$  is governed by the probability space  $(\Omega_1, \mathcal{F}_1, \mathbb{P}_1)$  only; it follows that  $\mathbb{E}_{\mathbb{Q}} [C_n]$  can be replaced by  $\mathbb{E}_{\mathbb{P}_1} [C_n]$ . On the other hand, note that

the expression  $(R_n FV + S)\mathbb{1}_{\tau > n}$  is governed by the probability space for the full model  $(\Omega, \mathcal{F}, \mathbb{Q})$ . Under  $\mathbb{Q}$  the indicator variable is assumed to be independent from the LIBOR rate. Moreover, the quantities  $FV$  and  $S$  are constants. Based on these remarks, the final expression in (3.13) can be further solved as follows:

$$\begin{aligned}
& \mathbb{E}_{\mathbb{Q}} [(R_n FV + S)\mathbb{1}_{\tau > n}] + \mathbb{E}_{\mathbb{Q}} [C_n] \\
&= \mathbb{E}_{\mathbb{Q}_2} [R_n FV + S] \mathbb{E}_{\mathbb{P}_1} [\mathbb{1}_{\tau > n}] + \mathbb{E}_{\mathbb{P}_1} [C_n] \\
&= \mathbb{E}_{\mathbb{Q}_2} [R_n FV + S] \mathbb{P}_1(\tau > n) + \mathbb{E}_{\mathbb{P}_1} [C_n] \\
&= FV \mathbb{E}_{\mathbb{Q}_2} [R_n] \mathbb{P}_1(\tau > n) + S \mathbb{P}_1(\tau > n) + \mathbb{E}_{\mathbb{P}_1} [C_n]
\end{aligned} \tag{3.14}$$

### 3.2.4 Monte Carlo Pricing

Assuming the expectation in (3.12) exists, the CAT bond price can be numerically approximated via Monte Carlo methods, in case there is no closed-form solution for equation (3.12). Indeed, by the law of large numbers, the higher the number of simulations, the closer the approximation to the true value, that is:

$$C_0 = \lim_{s \rightarrow \infty} C_0^{(s)} \tag{3.15}$$

where  $s$  denotes the number of simulations and  $C_0^{(s)}$  is obtained by averaging across all simulated outcomes, as shown below:

$$C_0^{(s)} = \frac{1}{s} \sum_{j=1}^s \sum_{n=1}^N B(n, r) [f_n^{(j)}(R_n^{(j)}, \tau^{(j)}) + C_n^{(j)}] \tag{3.16}$$

where  $f_n^{(j)}(\cdot)$ ,  $R_n^{(j)}$ ,  $\tau^{(j)}$ , and  $C_n^{(j)}$  denote the  $j$ -path realizations of  $f_n(\cdot)$ ,  $R_n$ ,  $\tau$ , and  $C_n$  respectively.

## 3.3 Assumptions

Aside from the independence assumption between financial market and insurance variables defined earlier in this chapter, the pricing model and the numerical study in Chapter 5 rely on the following restrictive assumptions.

### 3.3.1 Generalized Extreme Value Distribution

Under  $\mathbb{P}_1$ , the random variable  $I_t : \Omega_1 \rightarrow \mathbb{R}$  follows a generalized extreme value (GEV) distribution defined by the shape parameter  $\xi$ , the location parameter  $\mu$ , and the scale parameter  $\sigma$ :

$$I_t \sim GEV(\xi, \mu, \sigma) \quad (3.17)$$

The index continuous-time process  $(I_t)_{t \geq 0}$ , can be then discretized by  $\{I_{t_i}, i = 0, 1, 2, \dots\}$ , a sequence of iid and GEV distributed random variables. A comprehensive statistical framework about the GEV distribution and Extreme Value Theory is provided in Chapter 4, while a numerical application is provided in Chapter 5.

### 3.3.2 Geometric Brownian Motion

Following Romaniuk (2003) and Zimbidis et al. (2007), the LIBOR interest rate process  $(R_t)_{t \geq 0}$  is assumed to be driven by a geometric Brownian motion (GBM) under  $\mathbb{P}_2$ , the historical probability measure for financial market variables, according to the following stochastic differential equation (SDE):

$$\frac{dR_t}{R_t} = \mu^R dt + \sigma^R dW_t \quad (3.18)$$

where  $dR_t$  is the (random) instantaneous increment of  $R_t$ ,  $dt$  is the (deterministic) infinitesimal time interval,  $\mu^R$  and  $\sigma^R$  are the drift and volatility parameters respectively, and  $dW_t$  is the (random) instantaneous increment of  $W_t$ , a standard Brownian motion under  $\mathbb{P}_2$ . Equation (3.18) is the well-known solution to the SDE in (3.18).

$$R_t = R_0 \exp\left(\left(\mu^R - \frac{1}{2}(\sigma^R)^2\right)t + \sigma^R W_t\right) \quad (3.19)$$

Proof of the solution to the SDE can be found in Shreve (2004, p. 147-148). The above continuous equation can be approximated using a discrete scheme. Further details are provided in Chapter 5. Due to its simplicity and popularity, the GBM is chosen to model the stream of LIBOR cash flows. What makes the GBM attractive is the log-normality of the process, which is given by the Brownian

component. Other more advanced techniques, such as the CIR and Vasicek processes, retain the Brownian component and include the property of mean reversion. Nevertheless, a comparison of different interest rate processes is beyond the scope of this thesis.

### 3.3.3 No Arbitrage and Risk Neutral Pricing Measure

It is assumed that the market is arbitrage-free and hence there exists a risk-neutral pricing measure. The LIBOR is a financial market variable and its movements can be replicated by existing securities, such as interest rate derivatives. The LIBOR evolution is then modeled in a complete market framework and hence there exists a unique risk-neutral pricing measure  $\mathbb{Q}_2$  equivalent to  $\mathbb{P}_2$ . The LIBOR process can be converted from the historical to the risk-neutral probability measure by applying the Girsanov's theorem to the geometric Brownian motion in (3.19). According to the Girsanov's theorem, if  $W_t$  is a standard Brownian motion under  $\mathbb{P}_2$ , then  $\tilde{W}_t = W_t + \frac{\mu^R - r}{\sigma^R} t$  is a standard Brownian motion under  $\mathbb{Q}_2$ . The last identity can be rewritten in differential form as  $d\tilde{W}_t = dW_t + \frac{\mu^R - r}{\sigma^R} dt$ . Proof of these results can be found in Shreve (2004, p. 214-216). The dynamics of  $R_t$  can be then rewritten as follows:

$$\begin{aligned} \frac{dR_t}{R_t} &= \mu^R dt + \sigma^R dW_t \\ &= \mu^R dt + \sigma^R \left( d\tilde{W}_t - \frac{\mu^R - r}{\sigma^R} dt \right) \\ &= r dt + \sigma^R d\tilde{W}_t \end{aligned} \tag{3.20}$$

Hence, under the risk-neutral measure, the drift of the LIBOR return is simply the risk-free rate. Accordingly, the solution to the SDE becomes as illustrated below:

$$R_t = R_0 \exp \left( \left( r - \frac{1}{2} (\sigma^R)^2 \right) t + \sigma^R \tilde{W}_t \right) \tag{3.21}$$

While it is straightforward for financial market variables to switch from the actual to the risk-neutral measure, the same can not be said about insurance variables. Indeed, the underlying index is not linked to a tradable financial asset. This means that the market is incomplete, as movements in the underlying index can not be hedged by means of existing securities. Hence, the risk-neutral

measure can not be obtained by means of the replicating portfolio and it is not uniquely defined. Fortunately, however, the fact that natural catastrophes are largely uncorrelated to movements in financial markets makes the pricing easier than it would have been otherwise (Cox and Pedersen, 2000). Indeed, Lee and Yu (2002) argue that the index dynamics retain their original distributional characteristics when switching from the actual to the risk-neutral measure. The last statement can be justified under the Sharpe (1964) Capital Asset Pricing Model. Let  $\mathbb{Q}_1$  denote the equivalent martingale measure to  $\mathbb{P}_1$ , and let  $r^c$  denote the rate of return on the CAT bond. Assuming that  $\mathbb{Q}_1$  exists, equation (3.22) holds:

$$\mathbb{E}_{\mathbb{Q}_1} [r^c] = r \quad (3.22)$$

Let  $r^m$  denote the return on the market portfolio and  $\beta_c = \frac{\text{Cov}(r^c, r^m)}{\text{Var}(r^m)}$  the CAT bond's beta. The expected CAT bond return under the physical measure can be then expressed as follows:

$$\begin{aligned} \mathbb{E}_{\mathbb{P}_1} [r^c] &= r + \beta_c \mathbb{E}_{\mathbb{P}_1} [r^m - r] \\ &= \mathbb{E}_{\mathbb{Q}_1} [r^c] + \beta_c \mathbb{E}_{\mathbb{P}_1} [r^m - r] \end{aligned} \quad (3.23)$$

Assuming that  $\beta_c = 0$ , the expected CAT bond return is the same under the two different probability measures:

$$\beta_c = 0 \quad \iff \quad \mathbb{E}_{\mathbb{P}_1} [r^c] = \mathbb{E}_{\mathbb{Q}_1} [r^c] \quad (3.24)$$

An economic interpretation of (3.24) is that investors are neutral towards catastrophic risk; hence, the CAT bond expected return is simply the risk-free rate. Several contributions to the existing literature support this view. Lee and Yu (2002) claim that because catastrophic risk is unsystematic, the CAT bond expected return should not attach a risk premium. Similar arguments are provided by Vaugirard (2003a), adding that the overall economy is only marginally influenced by localized natural catastrophes and that investors are able to diversify away catastrophic risk by merely holding other usual financial instruments. Both papers base their conclusions on the idea that catastrophic events can be viewed as large discrete movements in the underlying index, known as *jumps*. Following the Merton (1976) model, it can be assumed that jump risk is unsystematic.

### 3.3.4 No Credit and Liquidity risk

CAT bonds are structured in a manner that the (in)solvency of the sponsor does not impact the repayment of the principal to the investor. However, to model these instruments as default-free, additional assumptions are required with respect to the SPV and the collateral account. It is assumed that the SPV cannot default on its contractual obligations toward the investor and that the principal invested in the collateral fund can be withdrawn, on demand, at its full nominal value. Moreover, in case the CAT bond is issued below par, i.e. the actual price paid by the investor to the SPV is lower than the face value, it is assumed that the remaining capital is provided by the sponsor, so that the principal remains fully collateralized.

## 3.4 Chapter Summary

From the investor's perspective, CAT bonds can be priced as contingent claims in an incomplete market framework under the key assumption that the LIBOR rate and the triggering index are independent random variables. The CAT bond price is the sum of the present values of expected future cash flows, which consist of coupon payments and principal redemption. The latter only depends on the triggering index, while coupon payments are sensitive to both the LIBOR rate (linear payoff) and triggering index (binary payoff). In case there is no closed-form solution to equation (3.12), the CAT bond price can be numerically approximated via Monte Carlo methods by averaging across all simulated cash flow streams as in (3.16). Based on the model assumptions, the simulated triggering index paths can be generated from the GEV distribution, whereas the simulation paths with respect to the LIBOR rate can be generated from a geometric Brownian motion.

# Extreme Value Theory

Extreme Value Theory (EVT) is a branch of statistics that deals with the behavior of rare and extreme events found in the tail of distributions. One of the aims of EVT is to predict values that lie well beyond the range of observable data. It finds applications in various fields of modern science, especially hydrology and meteorology. Aside from natural sciences, the statistics of extremes has drawn the attention of scholars and practitioners in the field of finance and insurance. This chapter introduces the reader to classical EVT, which addresses the limiting behavior of maxima. Most of the material covered in this chapter is based on the following textbooks:

1. Embrechts, Klüppelberg, and Mikosch (1997) (hereafter EKM)
2. Coles (2001)
3. McNeil, Frey, and Embrechts (2015, Ch. 5)

The applications of EVT on CAT bond pricing are thoroughly discussed in Chapter 5.

## 4.1 Identifying Extremes

To identify extreme values, there are two main approaches, namely *block maxima* method (BMM) and the *peak over threshold* (POT). The first method consists of dividing a time series into blocks of equal size and selecting the highest value of each block. Thus, a new series of block maxima is

created. The POT approach involves setting a (high) threshold and selecting all values that exceed this threshold. The distinction between these two approaches is of key importance because not only do the resulting sets of extreme values differ but they also follow two different classes of distribution functions. More specifically, block maxima follow a generalized extreme value distribution, whereas threshold exceedances follow a generalized Pareto. Gili and K ellezi (2006) argue that the POT approach uses data more efficiently than BMM. However, the same authors acknowledge the issue of data scarcity arising from the use of the POT method. Indeed, on the one hand, the threshold should be as high as possible to satisfy the asymptotic properties; but, on the other hand, a higher threshold reduces the number of observations (i.e. values exceeding the threshold) available for estimation. For this reason, in this thesis, the BMM path is chosen over the POT.

## 4.2 Fisher, Tippett, and Gnedenko Theorem

The Fisher and Tippett (1928) and Gnedenko (1943) convergence type theorem addresses the limiting distribution of block maxima. In the following theorem  $M_n$  denotes the maximum of a sequence of  $n$  independent and identically distributed (iid) random variables  $X_1, \dots, X_n$ . The following theorem is taken from Embrechts et al. (1999), while an extensive proof can be found in Coles (2001, Ch. 7).

**Theorem 4.1.** *(Fisher and Tippett, 1928; Gnedenko, 1943) Suppose  $X_1, \dots, X_n$  are independent and identically distributed random variables with distribution function  $F$ , and  $a_n > 0$ ,  $b_n$  are constants for some non-degenerate<sup>6</sup> limit distribution  $G$*

$$\lim_{n \rightarrow \infty} \mathbb{P}\left(\frac{M_n - b_n}{a_n} \leq x\right) = G(x) \quad x \in \mathbb{R} \quad (4.1)$$

Then  $G$  is one of the following types:

1. Fr chet

$$\Phi_\alpha(x) = \begin{cases} 0, & x \leq 0 \\ \exp(-x^{-\alpha}), & x > 0 \end{cases} \quad \alpha > 0 \quad (4.2)$$

<sup>6</sup> A non-degenerate distribution is one whose limiting distribution is not concentrated into a single point.

2. *Weibull*

$$\Psi_{\alpha}(x) = \begin{cases} \exp(-(-x)^{\alpha}), & x \leq 0 \\ 1, & x > 0 \end{cases} \quad \alpha > 0 \quad (4.3)$$

3. *Gumbel*

$$\Lambda(x) = \exp(-\exp(-x)) \quad x \in \mathbb{R} \quad (4.4)$$

In other words, theorem 4.1 states that the normalized block maxima  $\frac{M_n - b_n}{a_n}$  converge in distribution to a variable having a distribution within one of the three families listed above as the block size  $n$  increases.

### 4.2.1 Generalized Extreme Value Distribution

The three distribution functions in theorem 4.1 can be unified in one single function—the *generalized extreme value* (GEV) distribution. The generalized version has a three-parameter specification  $(\xi; \mu, \sigma)$ , where the three entries denote the *shape*, *location*, and *scale* parameters respectively. The GEV cumulative distribution function (DF) is determined as follows:

$$H_{\xi; \mu, \sigma}(x) = \begin{cases} \exp\left(-\left(1 + \xi z\right)^{-\frac{1}{\xi}}\right), & \xi \neq 0 \\ \exp(-\exp(-z)), & \xi = 0 \end{cases} \quad x \in \mathbb{R} \quad (4.5)$$

where  $z = \frac{x - \mu}{\sigma}$ ,  $\sigma > 0$  and  $1 + \xi z > 0$ . The GEV density (pdf) is obtained by differentiating the distribution function in (4.5). The resulting pdf is shown below:

$$h_{\xi; \mu, \sigma}(x) = \begin{cases} \frac{1}{\sigma} (1 + \xi z)^{-\frac{1}{\xi} - 1} \exp\left(-\left(1 + \xi z\right)^{-\frac{1}{\xi}}\right), & \xi \neq 0 \\ \frac{1}{\sigma} (\exp(-z)) \exp(-\exp(-z)), & \xi = 0 \end{cases} \quad x \in \mathbb{R} \quad (4.6)$$

The value of the shape parameter  $\xi$  indicates the class of the distribution. Indeed, the generalized representation reduces to one of the three classes of DF described in equations (4.2) to (4.4), depending on the value of  $\xi$ . There are three distinct cases:

1.  $\xi = \frac{1}{\alpha} > 0$  reduces to the Fréchet class (4.2)

2.  $\xi = -\frac{1}{\alpha} < 0$  reduces to the Weibull class (4.3)
3. The limiting case in which  $\xi = 0$  reduces to the Gumbel class (4.4), as already noticeable in equation (4.5)

In practice, neither the true value of the parameters  $(\xi, \mu, \sigma)$  nor their estimate  $(\hat{\xi}, \hat{\mu}, \hat{\sigma})$  is known ex-ante. Hence, the parameters need to be estimated from the available data. For this purpose the next section illustrate some popular estimation techniques within the EVT framework.

### 4.3 Inference on the GEV Distribution

This section discusses some of the most widely accepted estimation approaches in the context of EVT. Maximum likelihood and the Hill estimator are illustrated in detail. Other estimators are also briefly acknowledged, although a full comparison among different estimation techniques is beyond the scope of this thesis.

#### 4.3.1 Maximum Likelihood Estimation

The idea behind *maximum likelihood estimation* (MLE) is to maximize the likelihood function with the given available data. Intuitively, the likelihood function measures how plausible the parameters of a distribution are based on the evidence of the available data. MLE is an optimization problem, which consists of determining the values of a set of parameters that maximize the likelihood function. More formally, let  $\mathbf{x} \in \mathbb{R}^m$  be an  $m$ -element vector of observed data, and let  $\boldsymbol{\theta} \in \mathbb{R}^j$  be a  $j$ -element vector of the true (but unknown) parameters of a generic probability density function  $f(\mathbf{x} | \boldsymbol{\theta})$ . The likelihood function of  $\boldsymbol{\theta}$  given  $\mathbf{x}$  is defined as follows:

$$\mathcal{L}(\boldsymbol{\theta}; \mathbf{x}) = f(\mathbf{x} | \boldsymbol{\theta}) \tag{4.7}$$

Assuming the elements of  $\mathbf{x}$  are iid observations, equation (4.7) reduces to the following product structure:

$$\mathcal{L}(\boldsymbol{\theta}; \mathbf{x}) = \prod_{i=1}^m f(x_i | \boldsymbol{\theta}) \tag{4.8}$$

The computations can be further simplified by taking the natural logarithm on both sides of the above equation. Indeed, by switching from the level to the log specification, equation (4.8) can be converted from a product to a more convenient summation structure:

$$\log \mathcal{L}(\boldsymbol{\theta}; \mathbf{x}) = \log \left[ \prod_{i=1}^m f(x_i | \boldsymbol{\theta}) \right] = \sum_{i=1}^m \log f(x_i | \boldsymbol{\theta}) \quad (4.9)$$

Finally, the MLE estimate  $\hat{\boldsymbol{\theta}}$  is the value of  $\boldsymbol{\theta}$  for which the log-likelihood function is maximized. The last statement can be formalized in the equation (4.10):

$$\hat{\boldsymbol{\theta}} = \operatorname{argmax}_{\boldsymbol{\theta}} \{ \log \mathcal{L}(\boldsymbol{\theta}; \mathbf{x}) \} \quad (4.10)$$

The application of MLE requires an ex-ante sample of observed values as well as an assumption about the class of a pdf. In the context of classical EVT, the input data is that obtained by means of the BMM approach, while the pdf is the one defined in (4.6). The set of true, resp. estimated, parameters is denoted as  $\boldsymbol{\theta} = (\xi, \mu, \sigma)$ , resp.  $\hat{\boldsymbol{\theta}} = (\hat{\xi}, \hat{\mu}, \hat{\sigma})$ . In practice, no reasonable assumptions can be made about the sign of the shape parameter  $\xi$ , ex-ante. For this reason, it is best to apply MLE to the generalized representation rather than picking one of the three classes (Gilli and K ellezi, 2006). By combining (4.9) and the density in (4.6), the log-likelihood function of the GEV parameters is determined as follows:

$$\log \mathcal{L}(\xi, \mu, \sigma; \mathbf{x}) = \begin{cases} -m \log \sigma - (1 + \frac{1}{\xi}) \sum_{i=1}^m \log[1 + \xi z_i] - \sum_{i=1}^m [1 + \xi z_i]^{-\frac{1}{\xi}}, & \xi \neq 0 \\ -m \log \sigma - \sum_{i=1}^m z_i - \sum_{i=1}^m \exp(-z_i), & \xi = 0 \end{cases} \quad \mathbf{x} \in \mathbb{R}^m \quad (4.11)$$

where  $z_i = \frac{x_i - \mu}{\sigma}$ , provided that  $1 + \xi z_i > 0$ . Properties of the MLE estimator include consistency (i.e.  $\lim_{m \rightarrow \infty} \hat{\boldsymbol{\theta}} = \boldsymbol{\theta}$ ) and asymptotic normality. In the context of the GEV distribution, a study by Smith (1985) concluded that when  $\xi > -\frac{1}{2}$ , the MLE estimator retains its usual asymptotic properties.

### 4.3.2 Hill Estimator

Unlike the multivariate MLE estimator, the Hill (1975) approach only estimates the shape parameter  $\xi$  and its reciprocal  $\alpha$ . Before reading the estimation formula in (4.14), it is key to understand under

which conditions the Hill estimator applies. Hence, this section introduces the maximum domain of attraction (MDA) conditions before moving on to the Hill estimator and its properties.

Let  $\bar{F}(x)$  denote the right-hand tail of a generic distribution function  $F(x)$ , i.e.,  $\bar{F}(x) = 1 - F(x)$ . Consider the standard form of the Fréchet distribution  $\Phi_\alpha(x)$  in (4.2) and recall that  $\alpha > 0$ . Note that the Fréchet tail  $\bar{\Phi}_\alpha(x) = 1 - \exp(-x^{-\alpha})$  can be approximated by a power function for sufficiently large  $x$ , given that the two functions are asymptotically equivalent:

$$\lim_{x \rightarrow \infty} \frac{\bar{\Phi}_\alpha(x)}{x^{-\alpha}} = 1 \iff \bar{\Phi}_\alpha(x) \approx x^{-\alpha} \quad \text{as } x \rightarrow \infty \quad (4.12)$$

A generalization of the asymptotic behavior of  $\bar{\Phi}_\alpha(x)$  is represented by the following class of functions:

$$\bar{F}(x) = x^{-\alpha} L(x) \quad x > 0 \quad \alpha > 0 \quad (4.13)$$

For some slowly varying<sup>7</sup> function  $L(x)$ . Any distribution function  $F_\alpha(x)$ , whose tail behavior satisfies (4.13), is said to be in the *maximum domain of attraction* of the Fréchet distribution ( $F_\alpha \in \text{MDA}(\Phi_\alpha)$ ). In other words,  $\text{MDA}(\Phi_\alpha)$  represents a class of DF whose tail decays according to a power function. Aside from the Fréchet, the DF in this category include, but are not limited to, the Pareto, Student-t and log-gamma (McNeil et al., 2015, p. 140). Note that the other two types of GEV distribution do not belong to the Fréchet MDA, as the Gumbel DF has an exponentially decaying tail, while the Weibull has a finite right endpoint (see equations (4.4) and (4.3)).

The rate of decay  $\alpha = \frac{1}{\xi}$  is referred to as the *tail index* and can be estimated via the Hill (1975) method. Indeed, for any function  $F_\alpha \in \text{MDA}(\Phi_\alpha)$ , the Hill estimator for the tail index and the shape

<sup>7</sup> A Lebesgue-measurable function  $L(x)$  is *slowly varying* at  $\infty$  if it satisfies:

$$\lim_{x \rightarrow \infty} \frac{L(cx)}{L(x)} = 1 \quad c > 0$$

A Lebesgue-measurable function  $h(x)$  is *regularly varying* at  $\infty$  if it satisfies:

$$\lim_{x \rightarrow \infty} \frac{h(cx)}{h(x)} = c^\rho \quad c > 0 \quad \rho \in \mathbb{R}$$

**Remark:** If  $L(x)$  is slowly varying, then  $\bar{F}(x) = x^{-\alpha} L(x)$  is regularly varying. For further details, see McNeil et al. (2015, p. 139).

parameter is given as follows:

$$\hat{\alpha}_{k,m}^{hill} = \frac{1}{\hat{\xi}_{k,m}^{hill}} = \left( \frac{1}{k} \sum_{i=1}^k \log \frac{x_{(i)}}{x_{(k)}} \right)^{-1} \quad 2 \leq k \leq m \quad (4.14)$$

where  $\{x_{(i)}, i = 1, \dots, m\}$  is the sequence of the observed block maxima sorted in decreasing order  $x_{(1)} \geq x_{(2)} \dots \geq x_{(m)}$ . There are several ways to derive the Hill estimator (see EKM, Ch. 6); the most straightforward derivation can be found in McNeil et al. (2015, p. 158). EKM demonstrate that the tail index estimator is consistent, albeit biased, and asymptotically normal:

$$\sqrt{k}(\hat{\alpha}_{k,m}^{hill} - \alpha) \xrightarrow{d} \mathcal{N}(b(\alpha), \alpha^2) \quad (4.15)$$

where  $b(\alpha)$  denotes the size of the bias and  $\xrightarrow{d}$  denotes convergence in distribution, which is achieved when the following conditions hold:

1.  $k = k(m) \rightarrow \infty$  i.e. for a sufficiently large order statistic.
2.  $\frac{k}{m} \rightarrow 0$  as  $m \rightarrow \infty$  i.e. for  $k$  tending at infinity at a slower rate than  $m$ .

Similarly, de Haan and Peng (1998) show that the asymptotic distribution for the shape parameter estimator is as follows:

$$\sqrt{k}(\hat{\xi}_{k,m}^{hill} - \xi) \xrightarrow{d} \mathcal{N}(b(\xi), \xi^2) \quad (4.16)$$

The main challenge of the estimation via the Hill method is the choice of the order statistic  $k$ , which represents a trade-off between variance and bias. Indeed, for small level of  $k$ , the variance  $\frac{\xi^2}{k}$  is too large. On the other hand, large values of  $k$  increase the bias of the Hill estimator. It is generally recommended to select  $k$  by identifying a stable region in the Hill plot, which is the set of points  $\{(k, \hat{\xi}_{k,m}^{hill}), k = 2, \dots, m\}$ . However, Hill plots are notoriously volatile, and the search of a stable region can prove challenging. To address this issue, Resnick and Stărică (1997) propose an averaging technique to smooth the Hill plot and reduce the variance of the new estimator. This approach, although simple and obvious, proves effective in reducing the range of the plot and helps in identifying a stable region to choose  $k$  from. A more systematic method of threshold selection is proposed by Hall (1990) and later refined by Danielsson et al. (2001). This last approach selects the

level  $k$  that minimizes the asymptotic mean squared error (MSE). Given the sample size  $m$  and the auxiliary order statistic  $k_{aux,m} = 2\sqrt{m}$ , the MSE of the shape parameter estimator is given in (4.17).

$$\text{MSE}(m, k) = \mathbb{E} [(\hat{\xi}_{k,m}^{hill} - \hat{\xi}_{k_{aux,m}}^{hill})^2 | x_{(1)}, \dots, x_{(m)}] \quad (4.17)$$

The MSE is calculated numerically using bootstrapping replications of the original sample. Finally, the optimal level  $k_0$  is the solution to the following minimization problem:

$$k_0 = \underset{k}{\operatorname{argmin}} \text{MSE}(m, k) \quad (4.18)$$

### 4.3.3 Other Estimators

Other tail index estimators that apply under the Fréchet MDA conditions include Pickands (1975) and Dekkers, Einmahl, and De Haan (1989). These two estimators are compared against the Hill approach by de Haan and Peng (1998), and are found to have similar asymptotic properties. Other multivariate estimators for the GEV parameters include the Bayesian framework proposed by Coles (2001, Ch. 9), which requires a specification of a prior multivariate distribution for the set of GEV parameters without reference to data.

## 4.4 Chapter Summary

The statistical framework presented in this chapter determines a distribution of extreme values, which are defined as block maxima. Assuming that data obtained by means of the BMM approach are iid and GEV distributed, the distribution parameters can be estimated via maximum likelihood. Once the estimate of the shape parameter is known, the generalized representation reduces to one of the three types, which is determined by the Fisher, Tippett, and Gnedenko theorem. Provided that the Fréchet MDA conditions are satisfied, the shape parameter and the tail index can be obtained via an alternative method, namely the Hill estimator. One challenge of this approach is the selection of the optimal order statistic, which represents a typical trade-off between bias and variance. To address this issue Hall (1990) and Danielsson et al. (2001) propose a solution that minimizes the asymptotic mean squared error of the estimated shape parameter.

## Numerical Study

The following case study involves a recently completed CAT bond deal, and it is taken and adapted from Artemis.bm, a comprehensive provider of news, facts, and figures about CAT bonds as well as other Insurance-Linked Securities. The purpose of this case study is to determine a fair price of a CAT bond based on the following elements:

1. The pricing model developed in Chapter 3
2. The statistical framework presented in Chapter 4
3. Initial data from different sources

### 5.1 CAT Bond Deal

The Federal Emergency Management Agency (FEMA) is a United States government institution founded on April 1, 1979 via an executive order signed by President Jimmy Carter. Since its foundation, FEMA has coordinated the federal government's role in preparing for, preventing, mitigating the effects of, responding to, and recovering from all domestic disasters, whether natural or man-made. One of the mandates of FEMA is the administration of the National Flood Insurance Program, which provides affordable insurance to property owners in an attempt to reduce the impact of flooding on private and public structures. For the first time in its history, FEMA considers reducing the financial exposure of its flood insurance program by entering the CAT bond market. For this purpose, FEMA

**Table 5.1** – CAT bond deal summary. Source: Artemis (2018)

<b>FloodSmart Re Ltd. (Series 2018-1)</b>		
Tranche	Class A	Class B
Sponsor	FEMA	
SPV	Flood Smart Re Ltd.	
Attachment Point (USD billion)	7.5	5
Exhaustion Point (USD billion)	10	
Spread over LIBOR (p.a.)	11.5%	
Issuance date	July 31, 2018	
Maturity date	July 31, 2021	
Territory/Peril	US/Flood	
Trigger Type	Industry Loss Index	

approaches Flood Smart Re Ltd., a Bermuda-based company, to structure a CAT bond deal. The CAT bond contract structured by Flood Smart Re Ltd. functions as follows: The SPV sells the CAT bond, based on an industry loss trigger<sup>8</sup> and on flood events occurring anywhere in the United States (hereafter US/Flood), to investors in the two different tranches. Investors of both tranches would bear losses up to an exhaustion point ( $U^{AB}$ ) of \$10 billion. The Class A tranche bears an attachment point ( $K^A$ ) of \$7.5 billion, while the Class B tranche bears an attachment point ( $K^B$ ) of \$5 billion. The two tranches only differ in terms of the attachment point and are otherwise equivalent. The contract provides a three year single-event coverage to FEMA starting from July 31, 2018. In return, the federal agency is required to pay the SPV a yearly spread worth 11.5%<sup>9</sup> of the notional amount. The SPV, in turn, will transfer the spread payments to the investor along with yearly floating rate payments based on the 12-month LIBOR based on US Dollar (hereafter 12-Month USD LIBOR), generated from a risk-free collateral fund. Table 5.1 summarizes the FloodSmart Re Ltd. Series 2018-1 (hereafter FloodSmart) transaction sponsored by FEMA.

<sup>8</sup> In the original source provided by Artemis (2018), the CAT bond is based on an indemnity trigger. In this thesis however, the CAT bond has been adapted to an industry loss trigger for reasons of data availability.

<sup>9</sup> In the original source provided by Artemis (2018), the two tranches are supposed to be issued at par and differ in the spread. In this study however, it is assumed that both tranches pay the same spread and consequently differ in the price.

## 5.2 Objective and Methodology

The aim of this numerical study is to price the FloodSmart CAT bond from the perspective of an investor. The solution to this case study involves the following steps:

1. Gather historical data about US/Flood industry-wide losses. Using the BMM approach, derive a sequence of annual maxima. Adjust BMM loss data for inflation, if necessary.
2. Perform a Maximum Likelihood Estimation using the BMM data and assuming the industry loss index follows a GEV distribution. Discuss the accuracy the estimated GEV parameters.
3. Estimate the parameters of the GEV distribution via the Hill method. Compare this approach to the standard MLE optimization with the help of graphical tools. Select the most accurate fitted GEV model between the two.
4. Assuming the LIBOR rate is driven by a geometric Brownian motion, derive the average volatility from historical data and select an appropriate risk-free rate for the drift parameter. By means of a Monte Carlo simulation, determine the expected LIBOR rate at the end of each year.
5. Given the fitted GEV distribution obtained via the chosen approach, simulate the loss process and its impact on the CAT bond payoff. Finally, the price is obtained by averaging across all the simulated discounted payoffs, as shown in equation (3.16).
6. Based on the fitted GEV distribution, calculate the relevant risk measures associated with the industry loss index and its impact on the CAT bond payoff.
7. Summarize the key findings of the numerical analysis

## 5.3 Data

The initial data are obtained from the NatCatSERVICE of Munich Re. The data set comprises of 36 observations of US/Flood insured losses. Each observation is the annual maximum insured loss, in nominal terms, caused by a single US/Flood event. There is no need to filter the data via the

BMM approach, as this was already applied by Munich Re NatCatSERVICE in the first place. The data are adjusted for inflation as follows:

$$I_t = \frac{I_t^{nominal} \times 100}{CPI_t} \quad (5.1)$$

where  $I_t^{nominal}$  denotes the nominal industry loss at time  $t$ , as originally reported by Munich Re (2018),  $CPI_t$  denotes the Consumer Price Index at time  $t$ . The US Dollar based CPI annual values (CPALTT01USA661S) are obtained from Federal Reserve Economic Data (FRED), the database provided by the Federal Reserve Bank of St. Louis. Table 5.2 reports the full inflation-adjusted data set.

**Table 5.2** – Annual maximum US/Flood single-event insured losses (\$ billion). Inflation adjusted (in 2015 values). Sources: Munich Re (2018); Federal Reserve Bank of St. Louis (2018)

<b>Index</b>	<b>Year</b>	0.0870	1989	0.0228	1999	0.2935	2009
0.0518	1980	0.0507	1990	0.4085	2000	1.0537	2010
0.1043	1981	0.1149	1991	0.1417	2001	0.7742	2011
0.0123	1982	0.2079	1992	0.2008	2002	N/A	2012
0.3808	1983	2.0220	1993	N/A	2003	0.2340	2013
0.0502	1984	0.5893	1994	0.4491	2004	0.5406	2014
0.0551	1985	1.4028	1995	0.3410	2005	0.7000	2015
0.1233	1986	0.4362	1996	0.5144	2006	3.3576	2016
0.0581	1987	0.4838	1997	0.1431	2007	0.0774	2017
0.0325	1988	0.3441	1998	0.5524	2008		

The GEV model requires block maxima to be independent and identically distributed. A source of dependence may arise from inflation; however, to tackle this effect, the data have already been adjusted for inflation as in (5.1). Furthermore, by adopting blocks of large size, such as years, seasonality trends are largely eliminated (Gilli and K ellezi, 2006). Based on these considerations, there is no reason to doubt that the iid assumption is satisfied.

## 5.4 Maximum Likelihood Estimation

Using the package `qrmtools` from the statistical software R (R Core Team, 2014), it is possible to find the MLE estimates for the GEV distribution. The MLE algorithm returns the following set of estimated parameters:

$$\hat{\boldsymbol{\theta}} = (\hat{\xi}, \hat{\mu}, \hat{\sigma}) = (0.8657, 0.1387, 0.1557) \quad (5.2)$$

For which the likelihood is  $\log \mathcal{L}(\hat{\boldsymbol{\theta}}; \mathbf{x}) = -6.5958$ , and the covariance matrix of the parameters is given in (5.3). The covariance matrix is approximated via the Hessian of the log-likelihood function with respect to the GEV parameters. The detailed procedure can be found in the Appendix section B.

$$\mathbf{V}(\hat{\boldsymbol{\theta}}) = \begin{bmatrix} 0.06690741 & -0.002953476 & 0.0001916235 \\ -0.002953476 & 0.001039755 & 0.001044335 \\ 0.0001916235 & 0.001044335 & 0.001440196 \end{bmatrix} \quad (5.3)$$

By the properties of consistency and asymptotic normality, the MLE estimates follow approximately a multivariate normal with mean  $\boldsymbol{\theta}$  and variance  $\mathbf{V}$  (Coles, 2001). Given that  $\hat{\boldsymbol{\theta}} \sim \mathcal{N}(\boldsymbol{\theta}, \mathbf{V})$ , symmetric 95% confidence interval can be constructed for each parameter  $\hat{\theta}_i$  as follows:

$$\hat{\theta}_i \pm 1.96 \times \text{SE} \quad (5.4)$$

The parameters standard errors SE can be obtained as the square root of the diagonal elements of  $\mathbf{V}(\hat{\boldsymbol{\theta}})$ . Accordingly, table 5.3 reports the corresponding confidence intervals.

**Table 5.3** – 95% confidence intervals of the MLE estimates. Standard errors in parentheses. Source: personal research

Parameter	Estimate	Confidence interval	
		2.5%	97.5%
$\xi$	0.8657(0.2587)	0.3588	1.3727
$\mu$	0.1387(0.02645)	0.0755	0.2019
$\sigma$	0.1557(0.03358)	0.08128	0.23

From the above table, it is clear that the shape parameter is subject to a high degree of uncertainty, given a high SE and consequently a wide confidence interval. The high standard error can be attributed to the small sample size of available data. The next section considers an alternative approach—the Hill estimator for the shape parameter.

## 5.5 Hill Estimator

The Hill estimator requires the GEV distribution to be of the Fréchet type. Based on the MLE estimates in the previous section, there is sufficient evidence that the Fréchet MDA conditions are satisfied, as the confidence interval for  $\xi$  in table 5.3 does extend below 0. Moving on to the Hill approach, in an attempt to overcome the limitations of the MLE approach, the MLE estimate for the shape parameter is replaced by the Hill estimator. Once the Hill estimator is given, the MLE optimization is performed with respect to  $\mu$  and  $\sigma$ , taking  $\xi = \hat{\xi}_{k_0, m}^{hill}$  as given. The order statistic  $k$  and the corresponding Hill estimate are selected according to the Hall (1990) bootstrapping approach. Table 5.4 summarizes the outcome of the Hill estimation performed with respect to the shape parameter using the R package `tea`.

**Table 5.4** – Hill estimator. Threshold selection based on the Hall (1990) bootstrapping algorithm. Source: personal research

Sample size $m$	36
Bootstrapping replications	1000
Auxiliary order statistic $k_{aux}$	12
Optimal order statistic $k_0$	10
Estimated tail index $\hat{\alpha}_{k_0, m}^{hill}$	1.5261
Estimated shape parameter $\hat{\xi}_{k_0, m}^{hill}$	0.6553
Standard error of $\xi$	0.2072
95% Confidence interval	[0.2491, 1.0614]

The standard error in the above table is calculated as the square root of the asymptotic variance  $\hat{\xi}_{k_0, m}^{hill}/k_0$  based on the solution of de Haan and Peng (1998). Confidence interval are determined based

on the property of asymptotic normality. From the above table, it is clear that the Hill estimator produces a lower SE for the shape parameter and consequently a narrower confidence interval. For this reason, in this context, the Hill estimator is preferable to the MLE estimate for  $\xi$ . To estimate the remaining two parameters of the GEV distribution, the MLE optimization is repeated with respect to the parameters  $\mu$  and  $\sigma$ , taking  $\xi = \hat{\xi}_{k,m}^{hill} = 0.6553$  as given. The R package `evd` allows to perform MLE for the GEV distribution while keeping one or more parameters fixed. Table 5.5 reports the MLE estimates for  $\mu$  and  $\sigma$  with corresponding standard errors and 95% confidence intervals.

**Table 5.5** – Maximum likelihood estimation for location and scale parameter, with  $\xi = \hat{\xi}_{k,m}^{Hill} = 0.6553$ . Standard errors in parentheses. Source: personal research

Parameter	Estimate	Confidence interval	
		2.5%	97.5%
$\mu$	0.1502(0.03082)	0.08984	0.2107
$\sigma$	0.1593(0.03609)	0.08861	0.23

From the above table, it is interesting to note that the overall approach considerably reduces the standard error of the shape parameter but slightly increases those of the location and scale parameters. To further compare the two GEV models in terms of accuracy, the next section relies on graphical tools.

## 5.6 Diagnostic Plots

An informal, yet effective, method of assessing the accuracy of a fitted model is the use of graphical tools. For this reason, this section includes some relevant diagnostic plots for both fitted GEV models that were obtained via the two different approaches illustrated in the previous sections, namely the standard MLE algorithm and the Hill method (combined with MLE).

### 5.6.1 Density Plot

The density plot compares the empirical density, i.e. the actual density obtained by the data, against the theoretical probability density function given by the estimated parameters. Figure 5.1 provides

the density plot for both fitted GEV models.

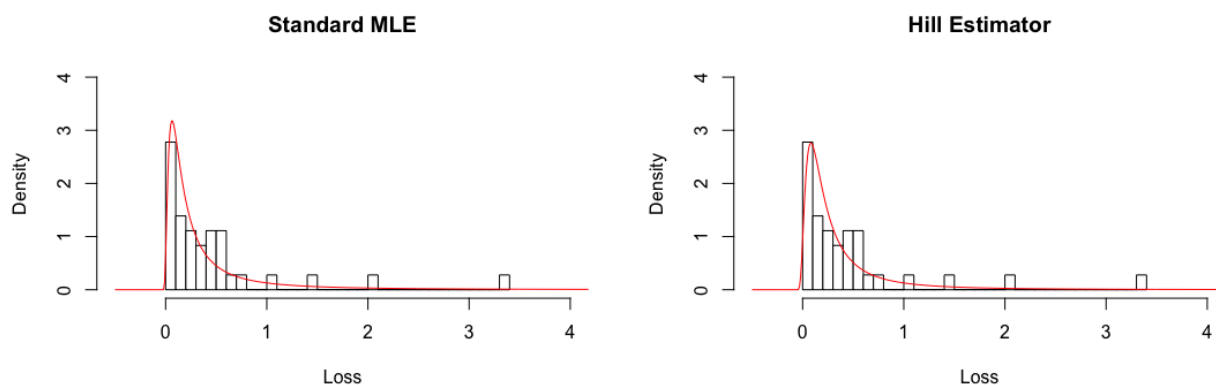


**Figure 5.1** – Empirical (histogram) and theoretical (red line) density functions, under standard MLE approach (left panel) and Hill estimator (right panel). Source: personal research

From the above chart, it appears that, in this context, the Hill approach is an improvement to standard MLE techniques. Indeed, in the right-hand panel, the theoretical density appears to better fit the histogram of actual data, given the lower height of the density function.

### 5.6.2 Distribution Plot

The distribution plot compares the theoretical cumulative distribution function against the empirical distribution given by the actual data. The distribution plot is provided in figure 5.2 for both fitted GEV models.

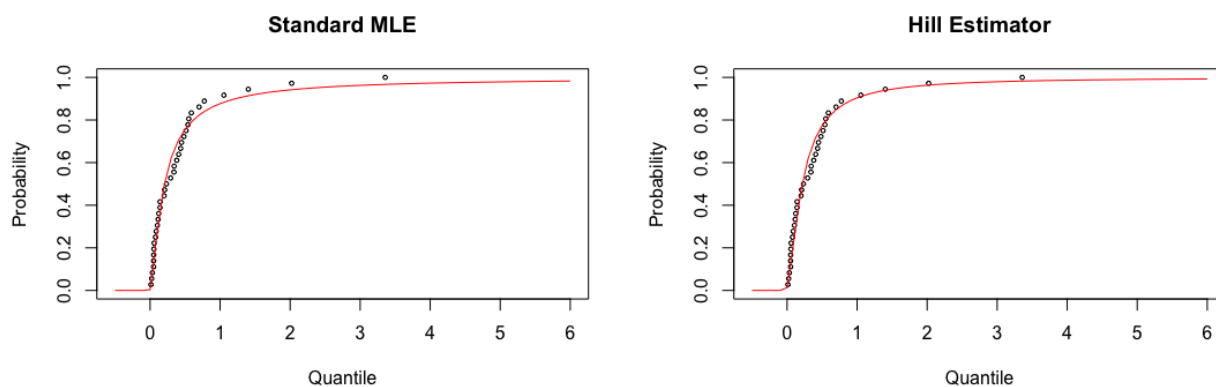


**Figure 5.2** – Empirical (set of points) and theoretical (red line) cumulative distribution functions, under standard MLE approach (left panel) and Hill estimator (right panel). Source: personal research

From the above chart, the Hill approach appears to better fit the actual data. In particular, both fitted models underestimate the probability of observing quantiles in the upper end. However, the error is considerably reduced when adopting the Hill estimator.

### 5.6.3 Q-Q Plot

Given the sequence of block maxima  $\{x^{(i)}, i = 1, \dots, m\}$  sorted in increasing order  $x^{(m)} \geq x^{(m-1)} \dots \geq x^{(1)}$ , and  $\left\{H_{\hat{\theta}}^{-1}\left(\frac{i}{m}\right), i = 1, \dots, m\right\}$ , the sequence of theoretical quantiles observable with probability  $\frac{i}{m}$ , the quantile-quantile (Q-Q) plot comprises of the following set of points:

$$\left\{\left(x^{(i)}, H_{\hat{\theta}}^{-1}\left(\frac{i}{m}\right)\right), i = 1, \dots, m\right\} \quad (5.5)$$

In other words, the Q-Q plot compares the observed (empirical) quantiles  $\{x^{(i)}, i = 1, \dots, m\}$  against those predicted by the fitted model via  $H_{\hat{\theta}}^{-1}$ , the inverse of the theoretical GEV distribution function  $H_{\hat{\theta}}$ . The highest accuracy is reached when the set of points perfectly aligns to a reference 45-degree line. Figure 5.3 includes the Q-Q plot for both fitted GEV models.

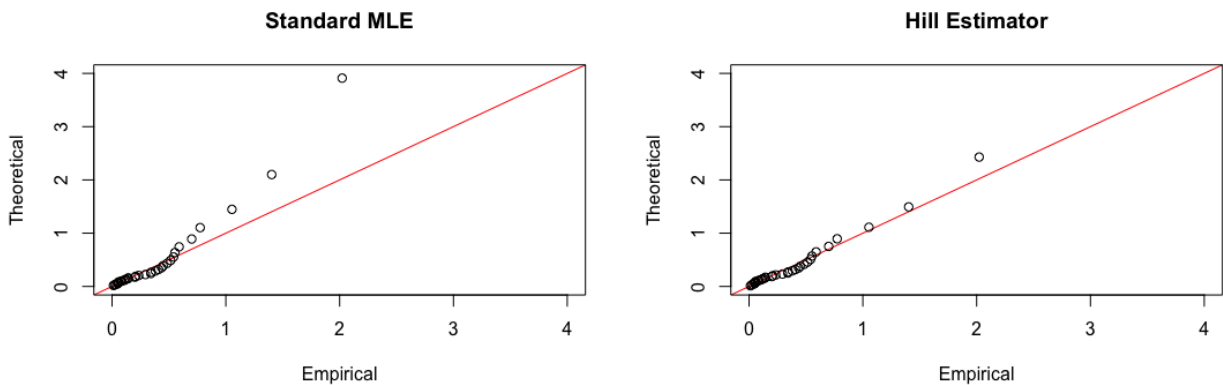


**Figure 5.3** – Q-Q plots under standard MLE approach (left panel) and Hill estimator (right panel). Source: personal research

From a visual inspection, the Hill approach appears to better predict quantiles. Both approaches overestimate quantiles in the upper range, although the error is smaller in the right-hand panel. As a final remark, note that the point  $\left\{\left(H_{\hat{\theta}}^{-1}(1), x^{(m)}\right), i = m\right\}$  is missing in both plots, as it is not finite.

### 5.6.4 Model Selection

Because of the lower standard error for the shape parameter and the better accuracy assessed from a visual inspection of the above diagnostic plots, the fitted GEV model based on the Hill estimator is chosen over the one obtained via standard MLE. Hence, the following sections of this numerical study rely on the distribution  $GEV(\hat{\xi}^{Hill} = 0.6553, \hat{\mu} = 0.1502, \hat{\sigma} = 0.1593)$ .

## 5.7 Monte Carlo Pricing

The first step of the risk neutral Monte Carlo pricing is the selection of the risk-free rate. The latter is assumed to be constant and plays two important roles in the simulation. First, it represents the drift of the LIBOR process, which is assumed to be driven by a geometric Brownian motion. Second, it is required to discount the cash flows of the CAT bond. The US 3-year treasury rate is chosen as a benchmark risk-free rate, which is equal to 2.77% as of July 31, 2018 (U.S. Department of the Treasury, 2019). Given that the industry loss index and the LIBOR rate are assumed to be driven by independent processes, they are simulated separately. First, the LIBOR rate is simulated according to a GBM, and the expected values at the end of each year are collected and added to the fixed spread payments of the CAT bond. This way, the full coupon payments for each year are obtained. Next, the industry loss index is simulated as a sequence of iid random variables along with its impact on coupon payments (binary payoff) and principal redemption (proportional payoff).

### 5.7.1 LIBOR

As established in chapter 3, the CAT bond coupons are sensitive to the LIBOR rate, which is assumed to be driven by a geometric Brownian motion. Under risk-neutral pricing, the drift of the GBM is the risk-free rate. Recalling equation (3.19), the solution to the GBM stochastic differential equation under the risk-neutral measure  $\mathbb{Q}_2$  is as follows:

$$R_t = R_0 \exp\left(\left(r - \frac{1}{2}(\sigma^R)^2\right)t + \sigma^R \tilde{W}_t\right)$$

In this numerical study, the above equation can be replaced by the following discrete approximation (Zimbidis et al., 2007):

$$R_{t+\Delta t} = R_t \exp\left(\left(r - \frac{1}{2}(\sigma^R)^2\right)\Delta t + \sigma^R \sqrt{\Delta t} \epsilon_t\right) \quad (5.6)$$

where  $\Delta t$  replaces  $dt$  and denotes a non-infinitesimal time interval, and  $\epsilon_t \sim \mathcal{N}(0, \Delta t)$  is a martingale under  $\mathbb{Q}_2$ . The sequential form in (5.6) is known as Euler scheme. The drift is the risk-free rate, while volatility, which is also assumed to be constant, can be estimated using historical data by taking the standard deviation from the series of the LIBOR relative increments. For this purpose, a daily time series of the 12-Month USD LIBOR (USD12MD156N) is downloaded from FRED. The sample period lasts 3 years (with 252 trading days per year), from July 31, 2015 to July 31, 2018. The length of the sample period reflects the maturity of the CAT bond. The standard deviation of the LIBOR increments from the time series, annualized via the square root rule, yields the following estimate for the volatility parameter:

$$\hat{\sigma}^R = 0.1114 \quad (5.7)$$

Using the R package `sde`, the LIBOR process can be simulated according to the Euler scheme in (5.6) with  $\Delta t = 1$ . The simulation is composed of 756 time steps (3 years of 252 trading days each) and 50,000 simulation paths. The starting value of the LIBOR rate is the last value of the historical series (on date July 31, 2018), which is  $R_0 = 0.02827$ . Given that the CAT bond pays LIBOR-based cash flows at the end of each year (i.e. on July 31, 2019, 2020, 2021), the simulated distributions at these dates are required to determine the CAT bond payoff from financial variables. From the simulated paths, the expected LIBOR rate at each year-end is shown below:

$$\mathbb{E}_{\mathbb{Q}_2}[\mathbf{R}] = (0.02907, 0.02989, 0.03073) \quad (5.8)$$

Where  $\mathbf{R} \in \mathbb{R}^3$  is a random vector denoting the realizations of  $R_t$  at the end of year 1, 2, and 3.

### 5.7.2 Industry Loss Index

The GEV assumption regarding the industry loss index implies that, in this framework, the values of the index are only extremes. This means that the ordinary values of the loss index are ignored. In classical EVT, extremes are defined as block maxima, and the block length is set at one year in this numerical study. In other words, the extremes of the loss process are expected to occur once per year. For this reason, the number of time steps in the Monte Carlo simulation is 3, as the CAT bond matures in 3 years. The number of simulated paths is 50,000. Accordingly, random numbers from the distribution  $GEV(\hat{\xi}^{Hill}, \hat{\mu}, \hat{\sigma})$  can be generated using the package **qrmtools**. The full coupon payments are obtained by summing expected values of the LIBOR payments, which result from a separate simulation algorithm, with fixed spread payments of \$11.50, based on a face value of \$100.00. Recall equations (3.15) and (3.16) from Chapter 3:

$$C_0 = \lim_{s \rightarrow \infty} C_0^{(s)}$$

$$C_0^{(s)} = \frac{1}{s} \sum_{j=1}^s \sum_{n=1}^N B(n, r) [f_n^{(j)}(R_n^{(j)}, \tau^{(j)}) + C_n^{(j)}]$$

The CAT bond price  $C_0$  can be numerically approximated as the average sum of discounted coupons and principal redemption across all the simulated scenarios. The Monte Carlo algorithm returns the price as **\$131.82** for Class A and **\$131.32** for Class B. As expected, the Class A tranche is more valuable than the Class B, given that the former has a higher attachment point than the latter. For a more comprehensive picture, the chart in figure 5.4 plots the FloodSmart CAT bond prices under different attachment points. Indeed, the CAT bond price increases monotonically with the trigger level, since the higher the threshold, the less likely the CAT bond is to be triggered. This implies a higher expected payoff, which is ultimately reflected in the price. However, the CAT bond price increment shrinks as the attachment point increases. This concave property can be explained by the fact that a higher trigger level reduces the gap between the exhaustion and the attachment point. Recalling from equation (3.6) that the ratio of principal redemption to the investor decreases proportionally with this gap, investors lose their principal more quickly once the CAT bond is triggered at higher thresholds.

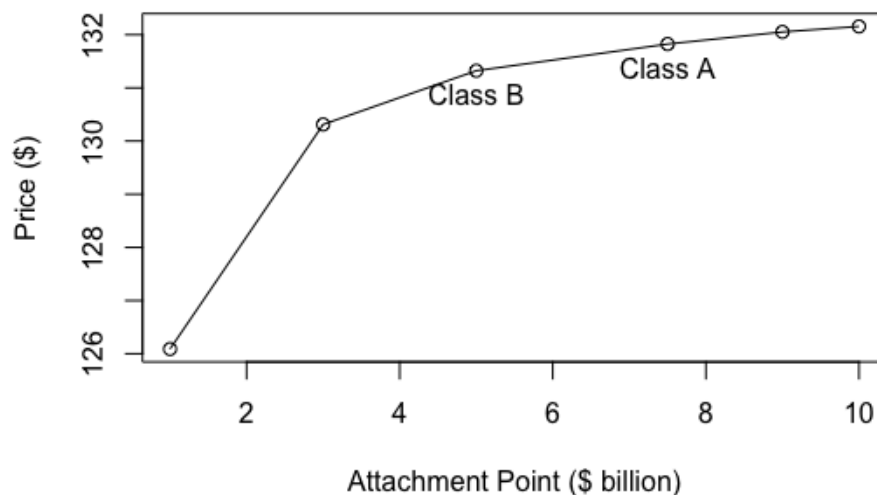


**Figure 5.4** – FloodSmart CAT bond price per \$100.00 of face value, evaluated at increasing attachment points (\$ billions) and exhaustion point of \$10 billion. Source: personal research

## 5.8 Risk Metrics

This section provides some key risk measures associated with the FloodSmart CAT bond based on the GEV distribution estimated in the previous section. Some values can be easily calculated via a closed-form solution, while others require Monte Carlo methods.

### 5.8.1 Exceedance Probabilities

To estimate the probability of both tranches being triggered, resp. exhausted, there is no need to rely on Monte Carlo methods. Indeed, given the fitted GEV model, the probabilities can be obtained via a closed-form solution. The probability of the industry loss index  $I$  exceeding a generic threshold  $u$  in one trial (i.e. within a 1 year period) is determined as follows:

$$\mathbb{P}_1(I_1 > u) = 1 - \mathbb{P}_1(I_1 \leq u) = 1 - H_{\hat{\xi}^{H+u}, \hat{\mu}, \hat{\sigma}}(u) \quad (5.9)$$

To determine the probability of the threshold being exceeded within a period of multiple years, recall that the index values are assumed to be iid. Based on this assumption, the probability of the index exceeding the threshold at least once within a period of  $m$  years is determined as follows:

$$\begin{aligned}
 & \mathbb{P}_1(\max(I_1, \dots, I_m) > u) \\
 &= 1 - \mathbb{P}_1(I_1, \dots, I_m \leq u) \\
 &= 1 - (\mathbb{P}_1(I_1 \leq u))^m \\
 &= 1 - (H_{\hat{\xi}^{Hill}, \hat{\mu}, \hat{\sigma}}(u))^m
 \end{aligned} \tag{5.10}$$

With reference to the pricing model in Chapter 3, setting the number of blocks  $m$  equal to the number of coupon dates  $N$ , and the last coupon date equal to the CAT bond's maturity  $T$ , the expression in (5.10) is equivalent to:

$$\mathbb{P}_1(\max(I_1, \dots, I_N) > K) = \mathbb{P}_1(\tau < T) \tag{5.11}$$

That is the probability of the CAT bond being triggered. The FloodSmart CAT bond has a maturity of 3 years, while extreme index values potentially exceeding the attachment point of \$5 billion, or even the exhaustion point of \$10 billion, are expected to occur once a year (BMM approach). The probabilities are then calculated accordingly over a period of 3 years. The value  $H_{\hat{\xi}^{Hill}, \hat{\mu}, \hat{\sigma}}(u)$  is computed using the package **qrmtools**. Table 5.6 reports the exceedance probabilities of the industry loss index over the 3-year horizon.

**Table 5.6** – Probability of exceeding the attachment, resp. exhaustion, points over multiple years, based on the distribution  $GEV(\hat{\xi}^{Hill} = 0.6553, \hat{\mu} = 0.1502, \hat{\sigma} = 0.1593)$ . Source: personal research

Threshold $u$ (\$ billion)	Exceedance probability		
	1 year	2 years	3 years
$K^B = 5$	0.009591726	0.01909145	0.02850006
$K^A = 7.5$	0.005225958	0.01042461	0.01559609
$U^{AB} = 10$	0.003387909	0.006764341	0.01012933

To interpret the above table with a few examples, the Class B tranche of the FloodSmart CAT bond is expected to be triggered within the first year of the contract, with a probability of 0.96%. Within the same year, the Class A tranche is less likely to be triggered, with a probability of 0.52%. Investors of both tranches should expect to lose the entire principal by the maturity date, with a probability of 1.01%.

### 5.8.2 Return Period

Closely related to the exceedance probabilities is the *return period*  $m(u)$ . The latter is defined as the expected number of blocks required to observe a loss, exceeding a threshold  $u$ . The return period is estimated as follows:

$$m(u) = \frac{1}{1 - H_{\hat{\xi}, \hat{\mu}, \hat{\sigma}}(u)} \quad (5.12)$$

The following table reports the return periods corresponding to the three relevant thresholds of the FloodSmart CAT bond according to the estimated GEV distribution.

**Table 5.7** – Return period based on the distribution  $GEV(\hat{\xi}^{Hill} = 0.6553, \hat{\mu} = 0.1502, \hat{\sigma} = 0.1593)$ , rounded to the nearest integer. Source: personal research

Threshold $u$ (\$ billion)	Return period $m(u)$
$K^B = 5$	104 years
$K^A = 7.5$	191 years
$U^{AB} = 10$	295 years

To interpret the above table with a few examples, the Class B tranche is expected to be triggered on average once within a period of approx. 104 years. As expected, the Class A tranche is safer, given the longer attachment period of approx. 191 years. Investors of both tranches would expect an event, which causes them to lose the entire capital, to occur on average once in approx. 295 years. In other words, the exhaustion point of \$10 billion can be interpreted as the one in 295 years loss, or the 295-year return level.

### 5.8.3 Expected Loss

While the two previous risk metrics pertain exclusively to the industry loss index, *expected loss* is focused on the impact that the index has on the principal redemption of the CAT bond. The CAT bond loss is calculated as the fraction of the principal that is transferred to the sponsor and hence lost by the investor. Forgone coupon payments are not accounted for when calculating losses, nor do accrued coupons compensate for losses in the principal redemption. The expected loss is the expected value of the difference between the full face value and the actual principal redemption. Based on equations (3.6) and (3.5) for the zero-coupon CAT bond, the expected loss EL per \$1 of face value can be derived as follows:

$$EL = \mathbb{E}_{\mathbb{P}_1} [p_\tau] \quad (5.13)$$

The *conditional expected loss* is defined as the expected loss, conditional on the CAT bond being triggered by the maturity date. In other words, it is the average loss incurred across all the scenarios in which the CAT bond is triggered. Recalling equation (3.6), the conditional expected loss CEL can be defined as follows:

$$CEL = \mathbb{E}_{\mathbb{P}_1} [p_\tau | \tau \leq T] \quad (5.14)$$

The expected and conditional expected loss are related to each other according to the following proposition:

**Proposition 5.1.** *Let  $EL = \mathbb{E}_{\mathbb{P}_1} [p_\tau]$  and  $CEL = \mathbb{E}_{\mathbb{P}_1} [p_\tau | \tau \leq T]$ , where the random variables  $\tau : \Omega_1 \rightarrow [0, \infty)$  and  $p_\tau : \Omega_1 \rightarrow [0, 1]$  are defined in (3.3) and (3.6) respectively. The following relation holds:*

$$EL = \mathbb{P}_1(\tau \leq T)CEL \quad (5.15)$$

*Proof.* See Appendix section A.

Hence, if either between EL and CEL is known, the other can be estimated closed-form. Nevertheless, both EL and CEL are estimated via Monte Carlo methods in this section. Table 5.8 reports the (conditional) expected losses for both tranches of the FloodSmart CAT bond, while the charts in

figure 5.5 plot the (conditional) expected losses across different attachment points.

**Table 5.8** – (Conditional) expected loss for the FloodSmart CAT bond. Source: personal research

Tranche	Attachment point $K$ (\$ billion)	EL	CEL
Class A	$K^A = 7.5$	1.25%	81.12%
Class B	$K^B = 5$	1.72%	59.09%

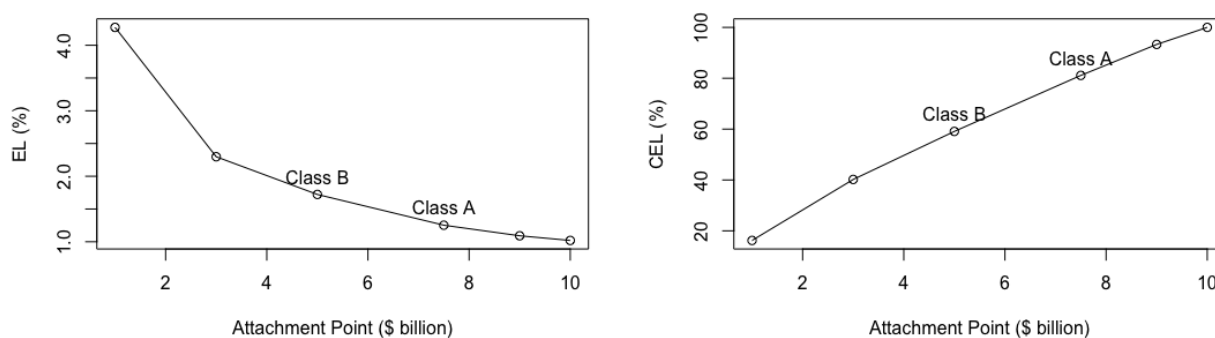


**Figure 5.5** – Expected loss (% , left panel) and conditional expected loss (% , right panel) of the FloodSmart CAT bond, evaluated at increasing attachment points (in \$ billion) and exhaustion point of \$10 billion. Source: personal research

From table 5.8 and the above charts, a clear pattern can be identified. As established in the previous subsection, the Class A tranche is less likely to be triggered than the Class B. This is ultimately reflected in the expected loss, which is accordingly lower for Class A. Indeed, the chart in figure 5.5 shows that the expected loss decreases with the attachment point. On the other hand, the conditional expected loss increases almost linearly with the attachment point, which would explain why the increment in the CAT bond value is diminishing as the attachment point increases in figure 5.4. It is again due to the fact that, at higher thresholds, the gap between the exhaustion and attachment point shrinks and so does the recovery rate of the principal, once the CAT bond is triggered.

### 5.8.4 Return Level

The *return level* is calculated with respect to the industry loss index. It is the loss that is expected to be exceeded on average once within a given number of blocks. For example, in the previous section, the return period of a loss of \$10 billion was estimated at approx. 295 years. Conversely, the 295 year return level corresponds to roughly \$10 billion. The return level is defined by the following GEV quantile function:

$$\hat{L}_m = H_{\hat{\xi}, \hat{\mu}, \hat{\sigma}}^{-1}\left(1 - \frac{1}{m}\right) = \hat{\mu} - \frac{\hat{\sigma}}{\hat{\xi}}\left(1 - \left(-\log\left(1 - \frac{1}{m}\right)\right)^{-\hat{\xi}}\right) \quad \hat{\xi} > 0 \quad (5.16)$$

Note that the return level should not be confused with the popular value at risk metric. Although both are quantile estimators, return level is a measure of maximum loss, a more conservative measure than value at risk (Gilli and K ellezi, 2006).

A return level plot of the function in (5.16) for the industry loss index is provided in figure 5.6. The plot shows the return level up to a number of blocks  $m = 300$  for the fitted GEV distribution.

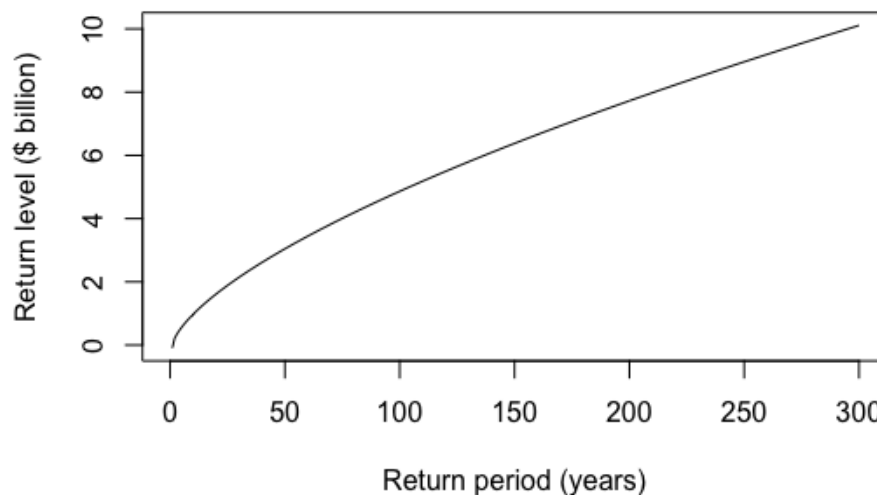


**Figure 5.6** – Return level plot based on the distribution  $GEV(\hat{\xi}^{Hill} = 0.6553, \hat{\mu} = 0.1502, \hat{\sigma} = 0.1593)$ . Source: personal research

The return level predictions should be accompanied by the corresponding confidence intervals.

This is however not possible in this study, since the covariance matrix of the parameters estimates is needed to determine the confidence interval (Coles, 2001, p. 56). In this approach however the covariances between the Hill estimator and the MLE estimates for  $\mu$  and  $\sigma$  can not be determined.

## 5.9 Chapter Summary

In this numerical study, two tranches of the FloodSmart CAT bond are priced by means of a Monte Carlo simulation, based on the pricing model developed in Chapter 3 and the statistical theory presented in Chapter 4. The two tranches have different attachment points but are otherwise equivalent. As anticipated, the tranche bearing a higher trigger level is safer (i.e. less likely to be triggered) and thus more valuable. This is further confirmed by the finding that Class A has a lower expected loss than Class B. In addition to the attachment points of Class A and B tranches, the Monte Carlo algorithm is replicated on other values for the threshold to determine price and (conditional) expected loss as a function of the attachment point. The outcome is graphically displayed in figures 5.4 and 5.5. This result further confirms the initial speculation that CAT bonds with higher triggering thresholds, maintaining everything else equal, are expected to be priced higher and bear a lower expected loss albeit a higher conditional expected loss. The key findings of this numerical study are summarized in table 5.9.

**Table 5.9** – Valuation summary. Source: personal research

<b>FloodSmart Re Ltd. (Series 2018-1)</b>		
Tranche	Class A	Class B
Estimated GEV parameters ( $\hat{\xi}^{Hill}, \hat{\mu}, \hat{\sigma}$ )	(0.6553, 0.1502, 0.1593)	
Attachment Point (\$ billions)	7.5	5
Attachment Probability (within 3 years)	1.56%	2.85%
Attachment Period (in years)	191	104
Exhaustion Point (\$ billions)	10	
Exhaustion Probability (within 3 years)	1.01%	
Exhaustion Period (in years)	295	
Expected Return (p.a.)	2.77%	
Expected Loss	1.25%	1.72%
Conditional Expected Loss	81.12%	59.09%
Spread over LIBOR	11.5%	
Price (per \$100 of Face Value)	\$131.82	\$131.32

## Conclusion and Further Research

This thesis successfully develops a general pricing framework for CAT bonds, which is consistent with no-arbitrage constraints. The contingent claim pricing model can be adjusted for pricing CAT bonds with different payoff structures. For example, in the pricing model, the principal redemption follows a proportional payoff; however, it can be simplified to a binary payoff structure by setting the attachment level equal to the exhaustion point. For simplicity, the LIBOR process was modeled as a geometric Brownian motion, and it would be interesting to switch to more advanced techniques such as the mean reverting CIR and Vasicek processes.

The numerical study is easily reproducible and can be replicated to evaluate other CAT bond deals based on natural catastrophe data, such as insured losses (both at industry and individual level) and physical parameters. In this study the Hill estimator for the shape parameter outperforms the MLE estimator owing to lower variance and better accuracy in terms of in sample forecasting. However, the same result is not guaranteed when replicating this study to other data. Furthermore, the Hill estimator should be applied only if there is sufficient evidence that the GEV distribution is of Fréchet type. It would also be interesting to compare the classical EVT approach employed in this study against one based on threshold exceedances. It would be then useful to assess whether the two models applied to the FloodSmart CAT bond produce similar results at an appropriate threshold selection for the POT approach.

# Bibliography

- Ammar, S., A. Braun, and M. Eling (2015). *Alternative Risk Transfer and Insurance-Linked Securities: Trends, Challenges and New Market Opportunities*, Volume 56. Institute of Insurance Economics IVW-HSG.
- Aon Securities (2018). Insurance-linked securities. *Report*.
- Artemis (2018). FloodSmart Re Ltd. (Series 2018-01). [http://www.artemis.bm/deal\\_directory/floodsmart-re-ltd-series-2018-1/](http://www.artemis.bm/deal_directory/floodsmart-re-ltd-series-2018-1/).
- Artemis (n.d.). What is a catastrophe bond (or cat bond)? <http://www.artemis.bm/library/what-is-a-catastrophe-bond.html>.
- Bodoff, N. and Y. Gan (2009, 01). An analysis of the market price of cat bonds. *Casualty Actuarial Society E-Forum*.
- Braun, A. (2012). Determinants of the cat bond spread at issuance. *Zeitschrift für die gesamte Versicherungswissenschaft* 101(5), 721–736.
- Braun, A. (2016). Pricing in the primary market for cat bonds: New empirical evidence. *Journal of Risk and Insurance* 83(4), 811–847.
- Coles, S. (2001). *An Introduction to Statistical Modeling of Extreme Values*, Volume 208. Springer.
- Cox, J. C., J. Ingersoll, and S. Ross (1985, 02). A theory of the term structure of interest rates. *Econometrica* 53, 385–407.
- Cox, S. H. and H. W. Pedersen (2000). Catastrophe risk bonds. *North American Actuarial Journal* 4(4), 56–82.
- Cummins, D. J. and M. A. Weiss (2009, 09). Convergence of insurance and financial markets: Hybrid

- and securitized risk-transfer solutions. *Journal of Risk and Insurance* 76, 493–595.
- Danielsson, J., L. de Haan, L. Peng, and C. G. de Vries (2001). Using a bootstrap method to choose the sample fraction in tail index estimation. *Journal of Multivariate Analysis* 76(2), 226–248.
- de Haan, L. and L. Peng (1998). Comparison of tail index estimators. *Statistica Neerlandica* 52(1), 60–70.
- Dekkers, A. L., J. H. Einmahl, and L. De Haan (1989). A moment estimator for the index of an extreme-value distribution. *The Annals of Statistics* 17(4), 1833–1855.
- Embrechts, P., C. Klüppelberg, and T. Mikosch (1997). *Modelling Extremal Events: For Insurance and Finance*. Berlin, Heidelberg: Springer-Verlag.
- Embrechts, P., S. I. Resnick, and G. Samorodnitsky (1999). Extreme value theory as a risk management tool. *North American Actuarial Journal* 3(2), 30–41.
- Federal Reserve Bank of St. Louis (2018, May). Federal Reserve Economic Data. <https://fred.stlouisfed.org/>.
- FEMA (n.d., May). About the Agency. <https://www.fema.gov/about-agency>.
- Fisher, R. A. and L. H. C. Tippett (1928). Limiting forms of the frequency distribution of the largest or smallest member of a sample. In *Mathematical Proceedings of the Cambridge Philosophical Society*, Volume 24, pp. 180–190. Cambridge University Press.
- Gilli, M. and E. Këllezi (2006). An application of extreme value theory for measuring financial risk. *Computational Economics* 27(2-3), 207–228.
- Gnedenko, B. (1943). Sur la distribution limite du terme maximum d’une serie aleatoire. *Annals of Mathematics*, 423–453.
- Hall, P. (1990). Using the bootstrap to estimate mean squared error and select smoothing parameter in nonparametric problems. *Journal of Multivariate Analysis* 32(2), 177–203.
- Hill, B. M. (1975). A simple general approach to inference about the tail of a distribution. *The Annals of Statistics*, 1163–1174.
- Hull, J. and A. White (1990). Pricing interest-rate-derivative securities. *The Review of Financial Studies* 3(4), 573–592.
- Jarrow, R. A. (2010). A simple robust model for cat bond valuation. *Finance Research Letters* 7(2), 72–79.

- Kunreuther, H. C. and E. O. Michel-Kerjan (2009). The development of new catastrophe risk markets. *Annual Review of Resource Economics* 1(1), 119–137.
- Lee, J.-P. and M.-T. Yu (2002, 05). Pricing default-risky cat bonds with moral hazard and basis risk. *Journal of Risk and Insurance* 69, 25–44.
- Lee, J.-P. and M.-T. Yu (2007). Valuation of catastrophe reinsurance with catastrophe bonds. *Insurance: Mathematics and Economics* 41(2), 264–278.
- Lombard Odier (2017). Rethink portfolio yield and diversification with insurance-linked securities. *Report*.
- McNeil, A. J., R. Frey, and P. Embrechts (2015). *Quantitative Risk Management: Concepts, Techniques and Tools-revised edition*. Princeton university press.
- Merton, R. (1976, 01). Option Prices When Underlying Stock Returns Are Discontinuous. *Journal of Financial Economics* 3, 125–144.
- Munich Re (2018, May). NatCatSERVICE. <https://natcatservice.munichre.com/>.
- Nowak, P. and M. Romaniuk (2013). Pricing and simulations of catastrophe bonds. *Insurance: Mathematics and Economics* 52(1), 18–28.
- Nowak, P. and M. Romaniuk (2018). Valuing catastrophe bonds involving correlation and CIR interest rate model. *Computational and Applied Mathematics* 37(1), 365–394.
- Pickands, J. (1975). Statistical inference using extreme order statistics. *The Annals of Statistics* 3(1), 119–131.
- R Core Team (2014). *R: A Language and Environment for Statistical Computing*. Vienna, Austria: R Foundation for Statistical Computing.
- Resnick, S. and C. Stărică (1997). Smoothing the Hill estimator. *Advances in Applied Probability* 29(1), 271–293.
- Romaniuk, M. (2003). Pricing the risk-transfer financial instruments via Monte Carlo methods. *Systems Analysis Modelling Simulation* 43(8), 1043–1064.
- Sharpe, W. F. (1964). Capital asset prices: A theory of market equilibrium under conditions of risk. *The Journal of Finance* 19(3), 425–442.
- Shreve, S. E. (2004). *Stochastic calculus for finance II: Continuous-time models*, Volume 11. Springer Science & Business Media.

- Smith, R. L. (1985). Maximum likelihood estimation in a class of nonregular cases. *Biometrika* 72(1), 67–90.
- Swiss Re (2011). The fundamentals of insurance-linked securities. *Report*.
- Swiss Re (2016, 07). Insurance-linked securities market update. *Market update*.
- Swiss Re (2018, 08). Insurance-linked securities market update. *Market update*.
- Towers Watson (2010). Catastrophe bonds evolve to address credit risk issues. *Report*.
- U.S. Department of the Treasury (2019). Daily Treasury Yield Curve Rates. <https://www.treasury.gov/resource-center/data-chart-center/interest-rates/pages/textview.aspx?data=yield>.
- Vasicek, O. (1977). An equilibrium characterization of the term structure. *Journal of Financial Economics* 5(2), 177–188.
- Vaugirard, V. E. (2003a). Pricing catastrophe bonds by an arbitrage approach. *The Quarterly Review of Economics and Finance* 43(1), 119–132.
- Vaugirard, V. E. (2003b). Valuing catastrophe bonds by Monte Carlo simulations. *Applied Mathematical Finance* 10(1), 75–90.
- Zimbidis, A., N. Frangos, and A. Pantelous (2007, 06). Modeling earthquake risk via extreme value theory and pricing the respective catastrophe bonds. *ASTIN Bulletin* 37, 163–184.

# Appendix

## A Proof of Proposition 5.1

Let  $EL = \mathbb{E}_{\mathbb{P}_1}[p_\tau]$  and  $CEL = \mathbb{E}_{\mathbb{P}_1}[p_\tau | \tau \leq T]$ , where the random variables  $\tau : \Omega_1 \rightarrow [0, \infty)$  and  $p_\tau : \Omega_1 \rightarrow [0, 1]$  are defined in (3.3) and (3.6) respectively. The following relation holds:

$$EL = \mathbb{P}_1(\tau \leq T)CEL \tag{5.17}$$

*Proof.* Let  $\{A_i, i = 1, 2\}$  be a finite partition of the sample space  $\Omega_1$  such that  $\{A_1 : \tau \leq T\}$  and  $\{A_2 : \tau > T\}$ . By the law of total expectations, EL can be expressed as the following sum:

$$EL = \mathbb{E}_{\mathbb{P}_1}[p_\tau] = \sum_i \mathbb{E}_{\mathbb{P}_1}[p_\tau | A_i] \mathbb{P}_1(A_i) \tag{5.18}$$

It follows:

$$\begin{aligned} EL &= \mathbb{E}_{\mathbb{P}_1}[p_\tau] \\ &= \mathbb{E}_{\mathbb{P}_1}[p_\tau | \tau \leq T] \mathbb{P}_1(\tau \leq T) + \mathbb{E}_{\mathbb{P}_1}[p_\tau | \tau > T] \mathbb{P}_1(\tau > T) \\ &= \mathbb{E}_{\mathbb{P}_1}[p_\tau | \tau \leq T] \mathbb{P}_1(\tau \leq T) && \text{(by definition of } p_\tau \text{ in (3.6))} \\ &= \mathbb{P}_1(\tau \leq T)CEL \end{aligned}$$

## B Approximation of the Covariance Matrix of the MLE Estimator

The R package `qrmtools` by Marius Hofert, Kurt Hornik, and Alexander J. McNeil approximates the covariance matrix of the MLE estimator for the GEV distribution as follows. First, it derives the Hessian matrix of the log-likelihood function. The Hessian matrix is the matrix of the second order partial derivatives of the log-likelihood function with respect to the GEV parameters. Let  $\ell = \log \mathcal{L}(\boldsymbol{\theta}; \mathbf{x})$ , then a generic element of the Hessian in (5.19) takes the following form:  $\mathbf{H}_{i,j}(\boldsymbol{\theta}) = \frac{\partial^2 \ell}{\partial \theta_i \partial \theta_j}$ .

$$\mathbf{H}(\boldsymbol{\theta}) = \begin{bmatrix} \frac{\partial^2 \ell}{\partial \xi^2} & \frac{\partial^2 \ell}{\partial \xi \partial \mu} & \frac{\partial^2 \ell}{\partial \xi \partial \sigma} \\ \frac{\partial^2 \ell}{\partial \mu \partial \xi} & \frac{\partial^2 \ell}{\partial \mu^2} & \frac{\partial^2 \ell}{\partial \mu \partial \sigma} \\ \frac{\partial^2 \ell}{\partial \sigma \partial \xi} & \frac{\partial^2 \ell}{\partial \sigma \partial \mu} & \frac{\partial^2 \ell}{\partial \sigma^2} \end{bmatrix} \times \ell \quad (5.19)$$

The elements of  $\mathbf{H}(\boldsymbol{\theta})$  evaluated at the corresponding MLE estimates yield the following matrix:

$$\mathbf{H}(\hat{\boldsymbol{\theta}}) = \begin{bmatrix} -30.27836 & -331.4788 & 244.395 \\ -331.4788 & -7169.102 & 5242.66 \\ 244.395 & 5242.66 & -4528.496 \end{bmatrix} \quad (5.20)$$

The observed information matrix is the negative of the MLE Hessian  $\mathcal{I}(\hat{\boldsymbol{\theta}}) = -\mathbf{H}(\hat{\boldsymbol{\theta}})$ . Finally, an approximate covariance matrix of the MLE estimates can be obtained via inversion of the observed information matrix:

$$\mathbf{V}(\hat{\boldsymbol{\theta}}) = \mathcal{I}^{-1}(\hat{\boldsymbol{\theta}}) = \begin{bmatrix} 0.06690741 & -0.002953476 & 0.0001916235 \\ -0.002953476 & 0.001039755 & 0.001044335 \\ 0.0001916235 & 0.001044335 & 0.001440196 \end{bmatrix} \quad (5.21)$$

## Eidesstattliche Erklärung

Der Verfasser erklärt an Eides statt, dass er die vorliegende Arbeit selbständig, ohne fremde Hilfe und ohne Benutzung anderer als die angegebenen Hilfsmittel angefertigt hat. Die aus fremden Quellen (einschliesslich elektronischer Quellen) direkt oder indirekt übernommenen Gedanken sind ausnahmslos als solche kenntlich gemacht. Die Arbeit ist in gleicher oder ähnlicher Form oder auszugsweise im Rahmen einer anderen Prüfung noch nicht vorgelegt worden.

.....

Ort, Datum

.....

Unterschrift des Verfassers